

**Report 90.161**

**Major fault zones within the Proterozoic  
Kautokeino Greenstone Belt, Finnmark,  
Norway: combined interpretation of  
geophysical data**

Rapport nr. 90.161		ISSN 0800-3416		Åpen/ <del>Forkastning</del>	
<p>Tittel:</p> <p>Major fault zones within the Precambrian Kautokeino Greenstone Belt, Finnmark, Norway: combined interpretation of geophysical data.</p>					
<p>Forfatter:</p> <p>Odleiv Olesen, Herbert Henkel, Ole Bernt Lile</p>			<p>Oppdragsgiver:</p> <p>Norsulfid/NTNF/NGU</p>		
<p>Fylke:</p> <p>Finnmark</p>			<p>Kommune:</p> <p>Kautokeino</p>		
<p>Kartbladnavn (M. 1:250 000)</p> <p>Nordreisa, Enontekiø, Karasjok</p>			<p>Kartbladnr. og -navn (M. 1:50 000)</p>		
<p>Forekomstens navn og koordinater:</p>			<p>Sidetall: 46</p>		<p>Pris: kr. 785,-</p>
<p>Feltarbeid utført:</p> <p>1989-1990</p>		<p>Rapportdato:</p> <p>18.03.1991</p>		<p>Prosjektnr.:</p> <p>61.1886.48</p>	
<p>Seksjonssjef:</p> <p><i>Jens S. Karvåg</i></p>					
<p>Sammendrag:</p> <p>Processed images of aeromagnetic, gravimetric and topographical data and geological maps combined with EM helicopter measurements and VLF ground measurements have been interpreted in mapping the main fault structures within the Kautokeino Greenstone Belt, KGB. The bulk of the mafic volcanic rocks in the Kautokeino Greenstone Belt is situated within a NNW-SSE-trending, 35 km wide and up to 5-6 km deep trough which is thought to represent an Early Proterozoic rift deformed by strike-slip faulting along the Bothnian-Kvænangen Fault Complex, BKFC. The margins of the Alta-Kautokeino Rift, AKR, can be outlined from the geophysical data. The Ciednjäljåkka-Boaganjav'ri Lineament and the Soadnjujav'ri-Bajasjav'ri Fault are the main bordering fault zones and are continuous along the entire greenstone belt. The supracrustals between these two zones are continuous to great depth (5-6 km) and the contacts along these bordering zones are steeply dipping. Gravity interpretations show that the outer amphibolite-facies rocks are just as deep as the central greenschist-facies unit. Results of the present study suggests that the amphibolite-facies volcano-sedimentary rocks at the flanks of the KGB should also be included in the rift.</p> <p>The mudstones and limestones in the Bik'kacákka Formation may have been formed during thermal subsidence as a result of cooling of upwelled asthenosphere after a phase of rifting. The above-lying deep and narrow Caravarri Formation contains abundant coarse-grained sandstones and conglomerates derived from a granitic source. We believe the Caravarri Formation to have been the result of late-stage uplift of the margins, subsequent erosion of the exposed basement, and deposition of the sediments in deep internal basins. Strike-slip movements may be incorporated in this model. Large-scale sinistral displacement along the BKFC embraced the AKR which was already a zone of weakness in the Karelian continental block. This strike-slip movement may have allowed the Caravarri Formation to form in a pull-apart basin within the rift.</p> <p>The 230 km long Mierujav'ri-Sværholt Fault Zone, MSFZ, is the main fault zone which separates the flat-lying volcanosedimentary sequences in the Masi area from the Jer'gul Gneiss Complex to the southeast. The MSFZ extends from Mierujav'ri 30 km north of Kautokeino in a northeasterly direction through Masi, Iesjav'ri and Lakselv and then beneath the Caledonian nappes on the Sværholt Peninsula. The correlative Galdenvarri and Vuomegielas Formations which represent the lowermost stratigraphical unit within the Kautokeino Greenstone Belt, are dextrally displaced 20 km along the MSFZ. The MSFZ is truncated by the eastern margin of the BKFC, and is thus interpreted to have been mainly active before the last major deformation of the rift. Proterozoic albite diabases, which cause characteristic magnetic anomalies in the Masi area, have intruded the MSFZ. Locally, younger deformation structures affecting these diabases can also be observed. A system of duplexes can be delineated along the MSFZ from the geophysical images. These interpretations have been followed up in the till-covered area with electromagnetic measurements and confirm the existence of the faults interpreted from the geophysical images. In the Masi-Iesjav'ri area breccias also occur along the MSFZ. Albite-carbonate alteration occurs along the borders of the Biggevarri Duplex. Folding and imbrication in the Masi-Iesjav'ri area is thought to be associated with movement along the MSFZ.</p>					
Emneord		Geofysikk		Magnetometri	
Berggrunnsgeologi		Gravimetri		Elektromagnetisk måling	
Forkastning		Petrofysikk		Prekambrium	
				Fagrapport	

## CONTENTS

1 INTRODUCTION .....	4
2 GEOLOGICAL SETTING .....	4
2.1 The Kautokeino Greenstone Belt .....	4
2.2 Regional fault zones .....	6
3 GEOPHYSICAL DATA .....	7
3.1 Aeromagnetic data .....	7
3.2 Gravity data .....	8
3.3 Electromagnetics .....	8
3.4 Digital topography .....	8
3.5 Petrophysical data .....	9
4 METHODS OF INTERPRETATION .....	9
4.1 Image processing .....	9
4.2 Structural interpretation .....	10
5 RESULTS .....	11
5.1 The Bothnian-Kvænangen Fault Complex .....	11
5.2 The Mierujav'ri-Sværholt Fault Zone. ....	13
6 DISCUSSION AND CONCLUSIONS .....	14
7 ACKNOWLEDGEMENTS .....	17
8 REFERENCES .....	17
LIST OF FIGURES .....	23
LIST OF PLATES .....	24
TABLES .....	25
Table 1. Rock densities applied in the gravity modelling .....	25
Table 2. Statistical data; density, susceptibility and Q-value for albite diabases .....	26
APPENDIX .....	27

Odleiv Olesen, Herbert Henkel\*, Ole Bernt Lile\*\*, Norges geologiske undersøkelse, P.O.Box 3006, N-7002 TRONDHEIM, \*Sveriges geologiska undersökning, P.O.Box 670, S-751 28 UPPSALA, \*\*Norges tekniske høgskole, N-7034 TRONDHEIM-NTH

## 1 INTRODUCTION

The purpose of this study has been to map the regional structures within the Kautokeino Greenstone Belt, KGB, (Siedlecka et al. 1985) in Finnmark, northern Norway. The main structural elements such as the Alta-Kautokeino Rift, AKR, (Bergh & Torske 1986), the Baltic-Bothnian megashear, BBMS, (Berthelsen & Marker 1986) which we suggest being named the Bothnian-Kvænangen Fault Complex, BKFC, and the Mierujav'ri-Sværholt Fault Zone, MSFZ (Olesen et al. 1990a) will be interpreted in more detail. The relationship between the MSFZ and the postglacial Stuoragurra Fault, SF, is outlined.

The Finnmarksvidda area is heavily covered with glacial drift. Regional digital aeromagnetic, electromagnetic, gravity and topographical data are therefore a necessary prerequisite to structural analysis. Compiled data-sets representing the Kautokeino-Masi area are presented in colour (Plates 1-3). High-frequency (spatial resolution) and shaded-relief images have proved particularly effective forms of enhancing information from regional data (Henkel et al. 1984, Henkel 1987, Lee et al. 1990). We have used image processing techniques to analyse and compare different types of data. For this purpose the magnetic dislocation map of Olesen & Solli (1985) has been transferred to the image processing system. The present study is a continuation of the interpretation by Olesen & Solli (1985) utilising improved techniques and more detailed data-sets.

The images of the more detailed data display, as expected, the previously recognised regional faults of the area (Olesen & Solli 1985). In the present study we will lay emphasis on delineating new interpretations on a regional scale from the Bothnian-Kvænangen Fault Complex and the Alta-Kautokeino Rift, and at a more detailed scale from the Mierujav'ri-Sværholt Fault Zone within the Masi area. In the latter area fault zones have to a large extent been controlled with ground measurements using the VLF-EM method. In the remaining area of the KGB, reconnaissance profiling and petrophysical sampling and *in situ* measurements were carried out.

As a consequence of the new interpretation fault-bounded borders of the AKR and duplex structures along the MSFZ have been identified. The present study also helps to resolve the ongoing controversy concerning the formation of the AKR, especially the extent of the rift within the KGB. Another intriguing question is to what extent the faulting is related to rifting or to the subsequent strike-slip deformation. Delineating the fault tectonics in the KGB also has a bearing on our understanding of the formation of gold deposits in the Bieddjuvaggi Mine and may be a valuable aid for the gold-exploration in adjacent areas.

## 2 GEOLOGICAL SETTING

### 2.1 The Kautokeino Greenstone Belt

The geological map of western Finnmarksvidda (Geological Surveys of Finland, Norway and Sweden

1987) is shown in Fig 1. The KGB comprises a 40-50 km wide synclinorium of Early Proterozoic volcano-sedimentary rocks (Solli 1983, Siedlecka et al. 1985, Krill et al. 1985, Olesen & Solli 1985, Olsen & Nilsen 1985, Hagen 1987). The KGB is situated between two culminations of gneisses, the Rai'sædno Gneiss Complex and the Jer'gul Gneiss Complex to the west and east, respectively (Fig. 1). These gneisses are partly of Archaean age (Olsen & Nilsen 1985) and form the basement to the greenstone belt. However, no clear depositional contact has been found between the gneisses and the supracrustals, presumably since the contacts are either fault-bounded or have been obliterated by younger felsic intrusions. The Rai'sædno Gneiss Complex may comprise partly remobilised Archaean gneisses (Olsen & Nilsen 1985) or migmatised equivalents of the Kautokeino Greenstone Belt. Opinions differ on the stratigraphy of the greenstone belt: from two cycles (Siedlecka et al. 1985, Solli 1983, Sandstad 1983, 1985, Olesen & Solli 1985, Hagen 1987) to four main volcanic cycles (Olsen & Nilsen 1985). We do not think that the evidence for the latter more complex stratigraphy is compelling and will therefore continue to advocate the former interpretation.

The Kautokeino Greenstone Belt can be subdivided into a number of formations. The oldest of these are the Gål'denvarri Formation (Solli 1983) and the correlative Vuomegielas Formation (Siedlecka (1985), which consists of mafic volcanic rocks metamorphosed in amphibolite facies. They have been found only along the eastern margin of the greenstone belt, to the south and northeast, respectively. The Masi Formation lies above the Gål'denvarri Formation with a supposed angular unconformity and consists of quartzitic rocks. The main body of the greenstone belt is occupied by the Cas'kejas, Suoluvuobmi and Lik'ca Formations (Siedlecka et al. 1985) each of which consists mainly of basic volcanites (Fig. 1). The volcanic rocks are dominated by basic tuff and tuffites, but basaltic lavas and concordant diabases are also present. Fine-grained clastic terrigenous sediments, mainly mica schists, are interbedded with the volcanites, but only in the Suoluvuobmi Formation to the northeast do they make up a considerable portion of the rocks. The Suoluvuobmi Formation in the Masi area is therefore interpreted to have formed on a platform at the margin of a rift. The youngest rocks of the greenstone belt are found in the central northern parts. Here it can be demonstrated that the volcanism in the Cas'kejas Formation gradually decreases and that the formation is concordantly overlain by pelites (Bik'kacåkka Fm.) and sandstones (Caravarri Fm.; Sandstad 1985). According to Bergh & Torske (1986, 1988) the Caravarri Formation and the greenschist-facies volcanosedimentary rocks within the eastern part of the Cas'kejas Formation were formed within the gradually subsiding Alta-Kautokeino Rift (AKR) along the margin of the Karelian continental block. We argue below that the whole of the Cas'kejas and Lik'ca Formations should be included in the AKR.

The western part of the Masi-Iesjav'ri area is occupied by the Suoluvuobmi and Lik'ca Formations (Siedlecka et al. 1985) which consist mainly of basic metavolcanites and metapelites. As seen from Fig. 1 and Plate 1 the general structural trend of this northeastern part of the KGB is NE-SW. Within this area both the bedding and the foliation are generally steeper to the east than to the west where the dip flattens out (Solli 1988). Deformation and metamorphism are of low intensity in the central parts of the KGB and increase towards the gneiss complexes to the west and to the east.

To the northwest, mudstones of the Upper Proterozoic/Lower Cambrian Dividal Group unconformably overlie the rocks of the greenstone belt. Above this are the Caledonian nappes which, in this area, consist mainly of feldspathic metasandstones.

## 2.2 Regional fault zones

The western area of the KGB is dominated by NNW-SSE trending faults interpreted by Olesen & Solli (1985). Berthelsen & Marker (1986) and Henkel (1988, in press) include these faults in the regional Baltic-Bothnian megashear and Bothnian-Seiland shear zone, respectively. We think that the name Bothnian-Kvænangen Fault Complex, BKFC, will be a more appropriate name since the zone can be traced from the Bay of Bothnia to Kvænangen. The complex is composed of several fault segments which are well defined from both geological and geophysical data (Holmsen et al. 1957, Olesen & Solli 1985, Berthelsen & Marker 1986, Geol. Surveys of Finland, Norway and Sweden 1986b, 1987, Henkel 1987, in press., Olesen et al. 1990a). The continuation further to the south into the Bay of Bothnia and the Baltic Sea is, however, less clearly defined. In the Kautokeino area 3-4 regional NNW-SSE fault zones have been delineated (Olesen et al. 1990a). Local faulting along these zones has been mapped by Holmsen et al. (1957). Berthelsen and Marker argue that movements along the BBMS consisted of a 160 km sinistral and subsequent 40 km dextral displacement during the period 1.9-1.8 Ga, based on offsets of the Sirkka line in northern Sweden and northern Finland.

Albite diabases have intruded one section of the BKFC bordering the eastern side of the Caravari Formation in the area of map-sheet Carajav'ri 1833 I (Solli 1990). The BKFC can be traced on aeromagnetic maps from the Finnmarksvidda area below the Caledonian nappes to the Raipas windows in Kvænangen (Olesen et al. 1990a). The western and eastern terminations of the Juv'ri Nappe, which is the lowermost unit within the Caledonian Nappe succession in western Finnmark (Sandstad 1985, Zwaan 1988), coincide with extensions of faults within the BKFC. This indicates that the BKFC was active during the Caledonian orogeny.

The 230 km long Mierujav'ri-Sværholt Fault Zone (MSFZ) extends from Mierujav'ri 30 km north of Kautokeino in a northeasterly direction through Masi, Iesjav'ri and Lakselv and then subsurface beneath the Caledonian nappes on the Sværholt Peninsula. In the Masi-Iesjav'ri area the MSFZ is parallel to the northwestern margin of the Jer'gul Gneiss Complex and is mostly situated within or at the border of the Masi Formation. Based on interpretation of aeromagnetic and gravity data the MSFZ truncates the Proterozoic Levajok Granulite Belt beneath the Caledonian nappes (Olesen et al. 1990a). The Archaean-Lower Proterozoic Gál'denvarri Formation and the correlative Vuomegielas Formation (Siedlecka et al. 1985) have been dextrally displaced 20 km along the MSFZ (Olesen et al. 1990a). In the Masi area, intrusions of  $1815 \pm 24$  Ma albite diabases (Krill et al. 1985) are related to the NE-SW trending MSFZ. The albite-diabases have a high magnetite content giving a characteristic anomaly pattern on aeromagnetic maps (Plates 1 & 5). To the southwest, the MSFZ is truncated by the Proterozoic BKFC. The MSFZ was therefore mainly active before the last major deformation of the Alta-Kautokeino Rift. Brecciation is common along the faults within both the BKFC and the MSFZ.

The Stuuragurra Fault, SF, (Olesen 1984, 1988b, Muir Wood 1989 and Olesen et al. 1990b) is situated within the MSFZ and is consequently parallel to the northwestern margin of the Jer'gul Gneiss Complex. The fault line is shown in Plate 4. It can be traced for 80 km, from Skarrejav'ri south of Masi in a northeasterly direction to Lævnjasjåkka northeast of Iesjav'ri. The fault is made up of numerous segments of faults with up to 10 m of reverse displacement. The SF is situated mainly within quartzites of the Masi Formation. North of Masi, however, the SF cross-cuts amphibolites within the Suoluvuobmi Formation and an albite diabase. Brecciation is observed in all the locations where the bedrock is exposed in the fault escarpment (Olesen et al. 1990b) and such brittle deformation is also observed along

the entire length of the MSFZ in the Precambrian on Finnmarksvidda. The brittle deformation is consequently believed to have occurred during the formation of the MSFZ and not the younger SF. So far, no ductile deformation has been observed along the MSFZ.

The earliest detectable displacements along the MSFZ are inferred to be Proterozoic (Olesen et al. 1990a) and the latest took place less than 9000 years ago (Olesen 1988, Olesen et al. 1990b). Along the MSF to the northeast of Iesjav'ri, a syn-sedimentary movement during the deposition of the Cambrian Dividal Group and a post/late-Caledonian displacement which cuts the Gaissa Thrust have been reported earlier (Townsend et al. 1989). Furthermore, the offshore extension of the MSFZ coincides with one of the major basement faults on the continental shelf (Lippard & Roberts 1987). The MSFZ must consequently represent an extremely long-lived fault-zone.

### 3 GEOPHYSICAL DATA

#### 3.1 Aeromagnetic data

The aeromagnetic measurements were carried out in two periods. In 1959-62 the area was drape-flown at an altitude of 150 m with a profile spacing of 1 km. Printed maps of the medium altitude data were published in the scale of 1:100,000 (Nor. geol. unders. 1981a,b,c,d) and 1:50,000. Maps in the scale of 1:50,000 have been digitised in a 500 x 500 m grid (Olesen et al. 1990a), from which the Definite Geomagnetic Reference Field 1965 was subsequently removed.

During 1979-85 most of the area was re flown at a profile spacing of 200-250 m and a flight altitude of 50 m (Håbrekke 1979, 1980a,b, 1981, 1983, 1984, Mogaard & Skilbrei 1986). These measurements are much more detailed than the former. The low-altitude surveys older than 1985 were compiled, levelled and interpreted by Olesen & Solli (1985), but because of confidentiality, only the interpretations were published. Skilbrei (1986) included the survey by Mogaard & Skilbrei (1986) in the compilation and levelled the data-sets using the 'orthognostic' mapping technique by Kihle (in prep.). In the present study an additional survey flown by Dighem (Dvorak 1982) on the 1:50,000 map sheet 1833 IV Mållejus has been included and the total of 29,000 profile-km of low-altitude measurements have been interpolated to a square grid of 100x100 m using the minimum curvature method (Briggs 1974, Swain 1976). The final grid was slightly smoothed using a 3 x 3 point Hanning filter. The data-set has been superimposed on the medium altitude 500 x 500 m grid to generate the coloured map shown in Plate 1. Because of the different flight altitudes, there are some discrepancies at the border of the medium- and low-altitude data-sets. The final map shown in Plate 1 has produced using the shaded relief technique (Lee et al. 1990, Kihle in prep.) with illumination from the east. The data from the Masi area are shown in Fig. 8.

### 3.2 Gravity data

The gravity map in Plate 2 is based on measurements from 2500 gravity stations. A regional gravity survey was carried out on Finnmarksvidda within the Finnmark Programme during the years 1980-1988 (Gellein 1985, Olesen & Solli 1985). Since 1985, 800 new gravity stations were measured within the area using snow scooter for transportation (Gellein 1990a,b). Measurements were made at approximately every 1 km along lines by 5-10 km apart. The complete Bouguer reduction (Mathisen 1976) of the gravity data has been computed using a rock density of  $2670 \text{ kg/m}^3$ , the International Gravity Standardization Net 1971 (I.G.S.N. 71) and the Gravity Formula 1980 for normal gravity. Another 250 measurements from Norges geografiske oppmåling (1979a,b) are included in the survey.

Since the grid was calculated at 500 m intervals the variable areal distribution of the primary observations has been homogenised by extracting stations with a minimum spacing of 300 m from the original data-set. This reduced data-set (ca. 2200 stations) was gridded using the minimum curvature method, and then smoothed using a 3 x 3 point Hanning filter. The final step in the process was to separate the data into a regional field associated with the mountainous Caledonian area to the northwest, and a residual component using the method by Olesen et al. (1990a). The contour interval of the residual field in Plate 2 is 1 mGal, and is believed to be larger than the error in the gravity data. The locations of the gravity stations are shown on the residual map. The data from the Masi area are shown in Fig. 9.

### 3.3 Electromagnetics

Electromagnetic data were collected during the helicopter-borne surveys (Håbrekke 1979, 1980a,b, 1981, 1983, 1984, Dvorak 1982, Mogaard & Skilbrei 1986). Discrete electromagnetic responses have been analysed to map conductors using the vertical sheet model. The conductance (i.e. conductivity-thickness product) in mhos of the vertical sheet model was calculated by computer in all of the surveys. This is done regardless of the interpreted geometric shape of the conductor. This was not an unreasonable procedure, because the computed conductance increases as the electrical quality of the conductor increases, regardless of its true shape. Strong conductors are characteristic of graphite or massive sulphides. Conductors with conductance higher than 5 mhos are plotted in Plate 4.

### 3.4 Digital topography

The Norwegian Mapping Authority (Statens kartverk, formerly named Norges Geografiske oppmåling) has provided a 100x100 m grid of digital topography from the area. This data-set was derived from digitised 1:50,000 scale topographical maps (M711 series), which had an original contour interval of 20 m. The use of digital topography in tectonic studies has been demonstrated by Henkel (1988). Glacial processes will enhance or obliterate pre-glacial tectonic imprints depending mainly on the direction and intensity of ice flow. The map shown in Plate 3 has been produced using the shaded relief technique



(Lee et al. 1990, Kihle in prep.) with illumination from the east. The data from the Masi area are shown in Fig. 10.

### 3.5 Petrophysical data

Olesen & Solli (1985) and Holst (1986) have reported petrophysical data for 1150 and 114 rock samples, respectively. An additional 1100 rock samples were collected during geological mapping and the follow up of geophysical anomalies (1986-1989). The rock samples (weighing 0.3 - 1.0 kg) have been measured with respect to density, magnetic susceptibility and remanent magnetisation. The measuring procedure is described by Olesen (1985) and Torsvik & Olesen (1988). The densities used in the gravity modelling are shown in Table 1. In addition, a large number of in situ determinations of magnetic susceptibility have been made in selected areas. These results are presented as histograms in Figs. 2 & 3. NRM measurements on rock samples of reversed magnetized diabase and albite diabase are shown in Fig. 4.

## 4 METHODS OF INTERPRETATION

### 4.1 Image processing

The data were analysed with an ERDAS image processing system (Erdas 1990a) running on an Olivetti M380 PC with an Intel 80386 processor and an IMAGRAPH 1024 x 1024 image processing card. The system can hold three raster images, each with a positive 8-bit range of 0-255 and one 4-bit graphic plane for overlays of vector data. The ERDAS system allows data to be swapped in and out of the image buffer and allows multiple data-sets to be easily compared.

The gridded gravity, aeromagnetic and topographical data-sets were rescaled into the 0-255 range. Histogram-equalised colour, high-frequency filtered and shaded-relief images have been used to enhance the information of the regional data-sets (Henkel et al. 1984, Gonzales & Wintz 1987, Lee et al. 1990). Shaded-relief presentations, which treat the grid as topography illuminated from a particular direction, have the property of enhancing features which do not trend parallel to the direction of illumination. The illusion of illumination (Figs. 5 & 6) is achieved by the application of two convolution filters of the form

$$\begin{array}{ccc} 1 & 0 & -1 \\ 1 & 0 & -1 \\ 1 & 0 & -1 \end{array} \quad \text{and} \quad \begin{array}{ccc} 1 & 1 & 1 \\ 0 & 0 & 0 \\ -1 & -1 & -1 \end{array}$$

to estimate the change in ground height in the X and Y directions. The dot product of the unit normal on the calculated surface and the sun vector gives a value representing the light reflectance. The interpretation of magnetic dislocations by Olesen & Solli (1985) and preliminary interpretations of

aeromagnetic data, the location of VLF ground profiles and VLF anomalies from the Masi area (Figs. 8, 9 & 10) have been digitised and transferred to the ERDAS system. These interpretations and the computed electrical conductors from the helicopter-borne electromagnetic measurements are represented as vector data in the image processing system.

The new structural analysis of the greenstone belt is subsequently performed by digitising the new interpretation elements directly on the video monitor using a mouse-controlled cursor. Both the updated interpretations and the previous ones are kept in the graphics plane while swapping the images from the three data sets. Once completed the final interpretation is plotted on top of the topographic map (Fig. 10 and Plate 4).

The preliminary interpretations in the Masi area were corrected as a consequence of the new information acquired from the enhanced images, and the final interpretation map is shown in Fig. 11.

#### 4.2 Structural interpretation

The structural interpretation utilising the image processing technique is similar to the method of Henkel et al. (1984) and Henkel (1987). In Henkel's method fault zones occurring within magnetic rock units are interpreted from: 1. Linear discordances in the anomaly pattern. 2. Displacement of reference structures. 3. Linear or slightly curved magnetic gradients. 4. Discordant linear or curved minima (Henkel & Guzmán 1977). The digital elevation data can be used to corroborate the interpretation of the magnetic data since fault zones commonly coincide with linear depressions in the topography. Regional fault zones will, furthermore, emerge as intermittent linear gradients in the gravity image.

Ground VLF and magnetic profiles with lengths varying from 400 m to 4 km have been measured on 28 selected locations across fault zones in the Masi area. The purpose of these measurements was to check and correct the interpretations based on the method just outlined. In regions of resistive soil and bedrock the VLF method can be used to detect large water-containing fracture zones in the bedrock (Henkel & Eriksson 1980, Eriksson 1980). The shape of the VLF-anomalies in the Appendix is compared with standard curves by Kaikkonen (1979) to estimate the dip of the conductors.

The magnetic banding within the KGB is generally found to represent primary layering of the volcanosedimentary sequences and metadiabase sills which now mostly show up with steep dips. The dip of albite diabases in the Masi area has been modelled using aeromagnetic data along helicopter-profiles and their measured magnetic properties. We have used a modified version (Hesselström 1987) of the computer programme by Enmark (1981) to compute the magnetic response of a model. The basic model in the programme comprises bodies of polygonal cross-section with limited extension in the strike direction. The susceptibilities of the highly magnetic albite diabases are shown in Table 2 and Fig. 3. For comparisons measurements from albite diabases in northern Sweden are included in Table 2. The albite diabases are thought to have intruded into the MSFZ and later been deformed due to movements along the fault zone.

Gravity modelling using the same software has been carried out along one profile across the Kautokeino

Greenstone Belt (Plate 2). The interpretation is shown in Profile A-C in Fig. 7. This profile is an extension of the profile interpreted by Olesen & Solli (1985) and is continuous across the whole of the greenstone belt. The densities used in the gravity modelling are shown in Table 1.

## 5 RESULTS

### 5.1 The Bothnian-Kvænangen Fault Complex

The NNW-SSE trending Alta-Kautokeino Rift is bounded to the west and east by steeply dipping fractures, the Ciednjaljåkka-Boaganjav'ri Lineament to the west, CBL, and the Soadnjujav'ri-Bajasjav'ri Fault, SBF, to the east (Plate 4). These structures are continuous along the entire greenstone belt and constitute part of the BKFC. Especially along the eastern fault, the SBF, cross-cutting relationships to magnetic reference structures can be observed. A striking feature seen in Plate 1 is the change in the magnetic pattern from NE-SW-trending structures 5 km north of Mierujav'ri to the NNW-SSE-trending structures at the margin of the AKR. This indicates that the NE-SW structures are transected by sinistral displacement along the SBF. Immediately to the south of the Caledonian front north of Soadnjujav'ri there is a similar discordance between the E-W-trending structures within the Suoluvuobmi Formation and the N-S-trending structures in the Lik'ca Formation. Holmsen et al. (1957) reported N-S-trending faults with brecciation and mylonitisation of the rocks at both locations. Further to the south, Olsen (in press) has reported shearing along this zone. A reversed magnetized dyke (Plates 1 & 4) has an apparent sinistral offset of 1 km along the SBF. The age of this dyke, based on palaeomagnetic studies, is 900-950 Ma (Mertanen et al 1990, S. Mertanen pers. comm. 1990). Measurements of natural remanent magnetisation on samples from this dyke are shown in Fig. 4B. Modelling of aeromagnetic profiles across this dyke shows that it dips 60-70° to the southeast. The true movement along the SBF after the intrusion of the dyke is therefore either (a) 1 km sinistral or (b) 2-3 km dip-slip with the eastern block being downthrown or (c) an oblique movement consisting of both sinistral and dip-slip movement.

The western zone, the CBL, appears on the aeromagnetic image as the border between the high-amplitude, banded magnetic pattern to the east and the low-amplitude, banded pattern to the west. The CBL coincide with the eastern margin of the migmatized Rai'sædno Gneiss Complex. This border is intruded by granites and pegmatites (Holmsen et al. 1957, Sandstad 1983, Olsen in press). However, faulting along the northern part of this lineament has been observed by Holmsen et al. (1957), and Sandstad (1983) reported strong deformation along this zone. Shear deformation has been observed by A. Bjørlykke (pers. comm. 1990) to the west of the Bieddjuvaggi Mine. Shear-heating at greater depth along strike-slip faults can enhance crustal anatexis (Michard-Vitrac et al. 1980, Sylvester 1988), and the original fault rock along the rift-fault may therefore not be recognisable. From the geophysical images, we conclude that the CBL represents the most distinct dislocation along the eastern border of the AKR. We interpret this lineament as a continuous fault zone from the better exposed area north of Rai'sjav'ri to the south. This southern area, which is to a great extent covered by glacial drift, a steep fault bordering the Rai'sædno Gneiss Complex has also been described by Holmsen et al. (1957, Fig. 16). Several large fault zones also occur within the rift (Plate 4). These, however, are not continuous along the entire rift. One interesting result is that the electrical conductors representing mainly graphite schists (Plate 4) seem to coincide with some of the fault zones which are interpreted from the aeromagnetic and

topographical data. Note that the VLF-EM method could not be used to control the location of these faults. These zones may represent the same type of shear zones as those appearing in the Bieddjuvaggi Mine which partly control the gold mineralisations within this mine (A. Bjørlykke pers. comm. 1990).

The gravity field in Plate 2 is composed of anomalies of different wavelengths. The central area, the Kautokeino Greenstone Belt, consists of alternating high and low, short-wavelength (5-10 km) anomalies. The local lows correspond to basement rocks, felsic intrusions and quartzites in antiforms, and sandstones within the basinal Caravarri Formation. The gravity highs correspond to the basic volcanites in the Cas'kejas, Lik'ca and Gål'denvarri Formations. Within the rift, both bedding and schistosity are generally steeply dipping. Flat-lying structures occur where the underlying basement forms dome structures (Olesen & Solli 1985). Four antiform structures in the Mierujav'ri area have been defined in addition to those previously identified by Holmsen et al. (1957) and Olesen & Solli (1985). These structures (Plate 4) can be interpreted either as gravitation-induced diapirs (Olesen & Solli 1985), as fold-interference phenomena (Olsen in prep.) or as shear-induced duplexes. The largest gravity highs are interpreted as accumulations of strongly folded and/or faulted amphibolites with depths of up to 6 km (Olesen & Solli 1985).

The western part of Profile A - C in Fig. 7 is dominated by a synclinorium of amphibolites from the Cas'kejas Formation. The volume of these rocks is significantly larger than that of the Gål'denvarri Fm. There is a prominent gravity low related to the Caravarri Formation. The mudstone underlying the Caravarri Formation is interpreted to have a depth of 5-6 km. Since the Caravarri Formation is deposited on top of the mudstone, the depth of these sandstones is likely to be similar. The depth of the Caravarri Formation, however, cannot be determined from the gravity data because of lack of density contrast with the underlying basement. The gravity data do not allow the presence of any greenstones below the Caravarri Formation.

From the aeromagnetic and gravity data, the AKR and the BKFC can be traced beneath the Caledonian nappes to the Alta-Kvænangen window, where they were deformed during the Caledonian orogeny (Zwaan & Gautier 1980, Olesen et al. 1990a). From the aeromagnetic and gravity maps by Olesen et al. (1990a) there is also evidence that the AKR continues further NNW onto the continental shelf of the Norwegian Sea.

Fig. 2 shows the frequency distributions of in situ susceptibility measurements of the main lithologies of the Cas'kejas Formation in the area of 1:50,000 map-sheet 1833 IV Mållejus. As described above, the eastern part of this map area contains mostly greenschist-facies rocks while the western part contains their amphibolite-facies equivalents (Sandstad 1983,1985). It has long been a matter of dispute whether or not these two units represent one and the same formation as stated by (Sandstad 1983,1985, Siedlecka et al. 1985), or two different units with regard to time of formation and depositional environment (Olsen & Nilsen 1985, Bergh & Torske 1988). The histograms in Fig. 2 show a very similar pattern for the correlative rock-types in the two areas. The bimodal distribution of the susceptibility is responsible for the typical banded anomaly pattern which can be seen within the AKR on the aeromagnetic map in Plate 1. There is no difference with regard to major element chemistry between the low-magnetic and the high-magnetic volcanites (Sandstad 1983). The difference in magnetite content must therefore be a result of different oxidation states inherited from the premetamorphic state (Grant 1985). The source of the volcanic rocks and the depositional environment is therefore likely to be similar in the two areas. In this context it should be pointed out that the Cas'kejas Formation is unique among the

volcanosedimentary formations in the Proterozoic on Finnmarksvidda in terms of high magnetite content. The aeromagnetic anomalies caused by the Cas'kejas Formation resemble those of the Kiruna and Kittilä greenstones in northern Sweden and northern Finland, respectively, with regard to amplitude and wavelength (Geological Surveys of Finland, Norway and Sweden 1986a).

## 5.2 The Mierujav'ri-Sværholt Fault Zone

The prominent, NE-SW-trending, characteristic high-magnetic anomalies in the Masi area are due to Proterozoic albite diabases that have intruded into faults within the MSFZ (see Plate 1). Outside this fault zone the albite diabases have intruded regionally as sills along layering and foliation surfaces. Locally, deformation of these diabases can be observed, for instance along the main road between Masi and Kautokeino (UTM coord. 602400-7698500) where the diabase has been transformed to amphibolite. From the aeromagnetic and topographical images a complex system of strike-slip duplexes (Woodcock & Fischer 1986) can be delineated along the MSFZ from Mierujav'ri to Iesjav'ri (Fig. 11 & Plate 4). Local, weak, magnetic anomalies are caused by small amounts of magnetite in quartzite beds within the Masi Formation. The interpretations have been followed up in the till-covered area with electromagnetic, VLF, ground profiles.

The VLF-profiles shown in the Appendix are located across the MSFZ (Fig. 11). The asymmetry of the VLF anomalies in the Appendix with a positive, high-amplitude, real component to the west and an accompanying negative, low-amplitude anomaly to the east indicates that the conductors generally dip to the east along the easternmost border of the MSFZ (Kaikkonen 1979, Lile & Singaas 1978). The difference between the positive and negative real component of the VLF anomalies is coded with symbols according to the legend in Fig. 11. The highest amplitude anomalies, indicated by crosses, are generally associated with the occurrence of graphite schists. The intersections along the postglacial Stuoragurra Fault (SF) are marked with arrows. In most of these profiles, the SF coincides with electrical conductors which are interpreted to be water-containing fracture zones (Fig. 11 & Appendix).

Magnetic model calculations along six aeromagnetic profiles are shown in Fig. 12. The dip estimates of the distinct magnetic anomalies are considered to be within  $\pm 5^\circ$ . The method, however, is not sensitive to the depth extent of thin and steeply dipping structures. The diabases in the models have therefore been truncated at approximately 1 km depth but they may be much deeper. The modelling of the dips along Profiles 390 and 140 indicates that the albite diabase has either intruded into a positive flower structure (Wilcox et al. 1973) or has been involved in the deformation along a similar structure. Figs. 11 and 12 show the dip determination of the diabases. The dip of the central albite diabase along the MSFZ varies from  $40^\circ$  SE in the Fidnajákka area to almost vertical at the Kautokeino River and to  $55^\circ$  NW further east of Masi. This 'twisting' of the albite diabase can also be observed on a more local scale along individual segments of the albite diabase along the MSFZ.

The wedge-shaped structure bordered by faults along Fidnajákka, Big'gejav'ri, Mazejákka and the Kautokeino River is interpreted as a contractional duplex which we propose to name the Biggevarri Duplex. A three-dimensional perspective model (Fig. 13) of the digital topography visualises the Biggevarri Duplex from the northeast.

In the eastern part of the gravity Profile A-C (Fig. 7) there is an increase in the regional field towards the Jer'gul Gneiss Complex. This long-wavelength anomaly is interpreted to be caused by a layered basement consisting of an upper acidic unit and a lower intermediate unit. On Finnmarksvidda, this layered basement is interpreted to form two large culminations with amplitudes of 5-7 km in the Rai'sædno and Jer'gul Gneiss Complexes as demonstrated by Olesen & Solli (1985). The western flank of the latter is visible on the profile. The gradient of the regional field is larger in the Masi area than in the Kautokeino area further to the south (Plate 2). The gravity anomaly caused by the Gål'denvarri Formation is situated on the flank of the regional anomaly.

According to the gravity modelling of Profile A-C in Fig. 7 the thickness of the Suoluvuobmi Fm. increases continuously to the west of the Masi Formation. The Biggevarri Duplex (Figs. 8 & 13) is therefore interpreted to continue underneath the amphibolites to the north of the Mazejåkka river. The albite-carbonate alteration along the Mazejåkka is thought to represent a gently northward-dipping roof of the Biggevarri Duplex structure mainly located within the quartzite. The Big'gejav'ri REE-Sr mineralization (Olerud 1988, Sandstad in prep.) located within an albitite is situated in the amphibolites shortly above this duplex interface and the mineralization may be related to faulting along the MSFZ.

The gravity low in Plate 2 to the northwest of Big'gejav'ri is caused by the absence of amphibolites in an anticlinal structure of quartzites of the Masi Formation. A magnetic anomaly (Plate 1) which is composed of short- and long-wavelength components, is related to the same structure, and is interpreted as sill-like intrusions of albite diabase, a relation that is generally valid in the Masi area (Olesen & Solli 1985). When interpreting the negative gravity anomaly in this area it was necessary to take into account the gravity effect of the amphibolites in the Suoluvuobmi Formation located 2 km to the north of Profile A-B (Fig. 1, Plate 2).

## 6 DISCUSSION AND CONCLUSIONS

The bulk of the mafic volcanites in the Kautokeino greenstone belt is located within a NNW-SSE-trending, 35 km wide and up to 5-6 km deep structure which is thought to represent the AKR modified by later folding, faulting and shearing along the BKFC. The borders of this sheared rift can be outlined from the geophysical images. The CBL and SBF in Plate 4 are the main bordering faults and are continuous along the whole of the greenstone belt. As can be seen from the three northernmost gravity profiles by Olesen & Solli (1985) the supracrustals between these two zones are continuous to great depth and the contacts along these bordering zones are generally steeply dipping. The southernmost profile in Olesen & Solli (1985) does not reveal a steep contact and is interpreted as the southern termination of the rift at the Finnish border. The quartzites within the Masi Formation along the Finnish border are characterised by their high metamorphic grade and migmatization (Olsen & Nilsen 1985). The high metamorphic grade is also characteristic further north at the western and eastern margins of the rift. We therefore favour the interpretation by Bergh & Torske (1984,1988) of a southward propagating rift into the Karelian continental block. Olsen & Nilsen (1985) and Bergh & Torske (1988) prefer to exclusively incorporate the low-grade volcanic rocks of the Cas'kejas Formation in the AKR. From the geophysical images there is no evidence of these low-grade rocks of the Cas'kejas Formation representing a separate fault-bounded rift. On the contrary, gravity interpretations by Olesen

& Solli (1985) and Fig. 7 show that the outer amphibolite-facies rocks are as deep as the central greenschist-facies unit. The present study consequently suggests that the amphibolite-facies volcano-sedimentary rocks at the flanks of the Kautokeino Greenstone Belt should also be included in the rift. Detailed mapping in the map area Mállejus by Sandstad (1983) shows that the two units represent the same stratigraphic succession with a gradual change in metamorphic facies from one unit to the other. Sandstad (1983) could not detect any abrupt break with regard to lithology, chemistry, metamorphism or tectonic style between the two units.

Bergh & Torske (1987) include the Bergmark area in the western part of the Alta-Kvænangen Window in the rift. The stratigraphy in this area (Vik 1981) is similar to the stratigraphy described by Sandstad (1983) for the westernmost part of the Cas'kejas Formation on the map-sheet Mállejus. This observation also supports our interpretation that the whole of the Cas'kejas Formation should be included in the rift.

The model for the development of the KGB must explain why the formation of the deep and narrow Caravarri Formation contains abundant coarse-grained sand and conglomerates derived from a granitic source (Holmsen et al. 1957, Siedlecka et al. 1985). This is most likely caused by late-stage uplift of the margins, subsequent erosion of the exposed basement and deposition of the sediments in deep internal basins. One model for the formation of the KGB was proposed by Olesen & Solli (1985); to re-establish gravitational equilibrium after the deposition of the dense volcanic rocks, the layered crust culminated on both sides of the belt and formed the Rai'sædno and Jer'gul Gneiss Complexes. In this late stage the uplifted basement was exposed to erosion and the sediments were deposited in basins within the greenstone belt. A similar model was proposed in northeastern Sweden by Lindroos & Henkel (1978). However, in this they incorporated marginal sedimentary basins and not a central basin.

An alternative model, following McKenzie (1978), involves the formation of the mudstones and limestones in the Bik'kacákka Formation during thermal subsidence as a result of cooling of upwelled asthenosphere after a phase of rifting. Specifically, horizontal heat flow could cause additional cooling within the rift and uplift of its shoulders (Ingersoll 1988). Strike-slip movements may be incorporated in the model. The large-scale sinistral displacement reported by Berthelsen & Marker (1986) and Henkel (1988) along the 1.9-1.8 Ga-old Baltic-Bothnian megashear embraced the 2.2-1.9 Ga Alta-Kautokeino Rift which was already a zone of weakness in the Karelian continental block. This strike-slip movement may have produced pull-apart basins within the rift. The Caravarri Formation has been interpreted to be the youngest unit within the greenstone belt. The strike-slip movements could also have triggered the formation of the gravity-induced diapirs which were delineated by Olesen & Solli (1985).

The flat-lying, thin (up to 2 km) sequences to the west of Masi (Fig. 1) are interpreted as having been deposited on a platform at the margins of the deep rift. This is supported by the increased volume of sediments in this area (Olesen & Solli 1985). The amphibolites occur adjacent to the AKR. The MSFZ constitutes the border between this flat-lying sequence to the northwest and the more deformed Gál'denvarri Formation and Jer'gul Gneiss Complex to the southeast (Fig. 1). Holmsen et al. (1957) and Solli (1983) reported that the Masi Formation has locally been inverted and thrust above the Suoluvuobmi Formation to the west. In the present model of the MSFZ we interpret the thrusting and imbrication of the Masi Formation to have occurred internally within the formation, as a result of dextral strike-slip movements along the MSFZ. The thrusting of the quartzite consequently developed mainly underneath and along the border of the Suoluvuobmi Formation.

In the area of map-sheet 1933 IV Masi (Solli 1988) foliation and layering steepen towards the Kautokeino river which, from the geophysical data, are interpreted to represent the central part of the MSFZ (Fig. 11). A palm tree structure (Sylvester & Smith 1976) slightly tilted to the northwest, can be inferred along the MSFZ by combining the geophysical interpretation and the geological observations. This type of structure typically occurs along strike-slip faults (Sylvester 1988). Two minor, fault-bounded blocks representing the Suoluvuobmi Formation on Árvusvarri and Háigadancákka (Solli 1988) are situated close to the centre of the MSFZ. These blocks are interpreted to be emplaced by normal faulting, which may represent extension across the top of the uplifted and laterally spreading blocks (Sylvester 1988). The S-shaped MSFZ, representing a restraining bend, is consistent with the observed accumulated dextral displacement of 20 km along the fault zone. The wedge-shaped positive Biggevarri Duplex interpreted from geophysical images may be formed as a consequence of this dextral strike-slip component. Internal thrusting of the Masi Formation within this structure was reported by Holmsen et al. (1957).

Based on the interpretation of aeromagnetic and gravimetric data the MSFZ truncates the Proterozoic Levajok Granulite Belt beneath the Caledonian nappes (Olesen et al. 1990a). On the Kola Peninsula a similar large-scale fault, the Mokhtozerkaya Fault Zone, MFZ (Barzhitzky 1988), has been reported to terminate the eastern end of the Lapland Granulite Complex which is the continuation of the Levajok Granulite Belt through Finland into the USSR. During or after the emplacement of the Levajok Granulite Belt in the continent-continent collision (Krill 1985), the MSFZ and the MFZ may have acted as dextral and sinistral transform faults, respectively. 'Indentor tectonics' (e.g. Tapponier et al. 1986) may also explain these large-scale strike-slip faults adjacent to continent-continent collision zones. Watterson (1978) suggested that indent-linked faults may be the main cause of the pervasive lineament networks in Precambrian continental crust.

Proterozoic albite diabases have intruded the MSFZ in the Masi area. Locally, deformation features can be observed in these diabases. In the Masi area Olesen (1988b) reported that the SF follows one old fracture zone and then cuts across to follow another. Interpretations of more detailed geophysical images have resulted in the delineation of a system of duplexes along the MSFZ from Mierujav'ri to Skoganvarre. Albite-carbonate alteration occurs along the borders of the Biggevarri Duplex. Slight tilting of the MSF towards the northwest may have been caused by the doming of the Jer'gul Gneiss Complex. Since the deformation increases towards the MSFZ the folding and imbrication in this area may be associated with movement along the MSFZ.

To the southwest into northern Sweden, an extension of the MSFZ can be found; the Karesuando-Arjeplog Fault Zone, KAFZ (Fig. 14), reported by Henkel (in press). This fault zone occurs in the Tjärrå Formation which is correlated with the Masi Formation (Geol. Surveys of Finland, Norway and Sweden 1987) and is intruded by highly magnetic albite diabases. The MSFZ and KAFZ have an apparent sinistral offset of 10-15 km along the BKFC (Fig. 14).

The postglacial Stuoragurra Fault, SF, is situated within the MSFZ and is governed by older faulting, on a local (Olesen et al. 1990b) as well as on a regional scale. Postglacial faulting occurs most commonly along the margins of or within the duplex structures. Northeast of Iesjav'ri, however, the young faulting occurs within the main fault zone. The earliest detectable displacement is of Proterozoic age and the latest took place less than 9000 years ago (Olesen 1988). Furthermore, seismicity occurs along an elongated tract oriented NE-SW nearly parallel to the neotectonic structures, with an approximately 30



km offset to the southeast. This indicates that the forces, which produced the faulting, may still be active.

## 7 ACKNOWLEDGEMENTS

This work was partially financed by Norsulfid as, the Royal Norwegian Council for Scientific and Industrial Research, NTNF (Grant 13220 to Odleiv Olesen), the Geological Survey of Norway and the Norwegian Institute of Technology, University of Trondheim. The study benefitted from collaboration with the NTNF project 'Ore genesis within the Kautokeino Greenstone Belt' conducted by Professor Arne Bjørlykke at the University of Oslo. The gravity measurements and much of the petrophysical laboratory work have been performed by several colleagues within the Finnmark Programme and the Geophysical Department of the Geological Survey of Norway. Jan Sverre Sandstad, David Roberts, Arne Solli, Trond Torsvik and Professors Roy Gabrielsen and Christopher Talbot have contributed with valuable discussions. To all these persons and institutions we express our sincere thanks. We are also indebted to David Roberts, Jan Sverre Sandstad and Peter Walker for critically reading the manuscript and for suggestions towards its improvement. We are further grateful to Randi Blomsøy, Gunnar Grønli and Bjørg Inger Svendgård for preparing the figures.

## 8 REFERENCES

- Barzhitzky, V.V. 1988: Kosmogeologicheskaya karta, Dochertvertichnyh obrasovaniy, Servero-vostochnoy chasti Baltiiskogo shtshita, Masshtab 1:1 000 000, ob'yasnitel'naya zapiska. Ministerstro geologii SSSR, Kiev, 86 pp.
- Bergh, S.G. & Torske, T. 1986: The Proterozoic Skoadduvarri Sandstone Formation, Alta, northern Norway: A tectonic fan-delta complex. *Sediment. Geol.* 47, 1-25.
- Bergh, S.G & Torske, T. 1988: Palaeovolcanology and tectonic setting of a Proterozoic metatholeiitic sequence near the Baltic Shield margin, northern Norway. *Precambrian Res.* 39, 227-246.
- Berthelsen, A. & Marker, M. 1986: 1.9-1.8 Ga old strike-slip megashears in the Baltic Shield, and their plate tectonic implications. In: D.A. Galson & S. Mueller (Eds.), *The European Geotraverse, Part 2. Tectonophysics* 128, 163-181.
- Briggs, I.C. 1974: Machine contouring using minimum curvature. *Geophysics* 39, 39-48.
- Dvorak, Z. 1982: DIGHEM<sup>II</sup> survey of the Finnmark area, Norway for A/S Sydvaranger. Dighem Ltd. Report 706, 69 pp.
- Enmark, T. 1981: A versatile interactive computer program for computation and automatic optimization of gravity models. *Geoexploration* 19, 47-66.

- Erdas 1990a: Image processing module, version 7.4, January 1990. ERDAS Inc., Atlanta, USA. 217 pp.
- Erdas 1990b: 3D module, version 7.4.1, August 1990. ERDAS Inc., Atlanta, USA. 12 pp.
- Eriksson, L. 1980: Elektriska och magnetiska metoder för påvisande av svaghetszoner i berg (Abstract in English). Unpublished Geophysical Report, Sveriges geologiska undersökning, SGU, 8012. 17pp.
- Gellein, J. 1985: Gravimetrisk Bougueranomali kart, Finnmarksvidda, M 1:250 000. Unpubl. NGU report 85.179, 11 pp.
- Gellein, J. 1990a: Bouguer gravity anomaly map, Enontekiö 1:250,000. Nor. geol. unders.
- Gellein, J. 1990b: Bouguer gravity anomaly map, Nordreisa 1:250,000. Nor. geol. unders.
- Geological Surveys of Finland, Norway and Sweden 1986a: Aeromagnetic anomaly map, Northern Fennoscandia, 1:1 mill, Helsinki. ISBN-91-7158-375-0.
- Geological Surveys of Finland, Norway and Sweden 1986b: Aeromagnetic interpretation map, Northern Fennoscandia, 1:1 mill, Helsinki. ISBN-91-7158-376-9.
- Geological Surveys of Finland, Norway and Sweden 1987: Geological map, Northern Fennoscandia, 1:1 mill, Helsinki. ISBN-91-7158-370-X.
- Gonzales, R.C. & Wintz, P. 1987: Digital image processing. Addison-Wesley Publishing Company. Reading, Massachusetts, USA, 503 pp.
- Grant, F.S. 1985: Aeromagnetism, geology and ore environments, I. Magnetite in igneous, sedimentary and metamorphic rocks: an overview. *Geoexploration* 23, 303-333.
- Hagen, R. 1987. Kautokeino grønnsteinsbelte, Unpubl. bedrock geology map 1:100.000. A/S Prospektering, Oslo.
- Henkel, H. 1979: Dislocation sets in northern Sweden. *Geol. För. Stockholm Förh.* 100, 271-278.
- Henkel, H. 1984: Nordkalottprojektet - flygmagnetisk tolkning i testområdet. Unpubl. SGU report 84.04, 22 pp.
- Henkel, H. 1988: Tectonic studies in the Lansjärv region. Svensk kärnbränslehantering AB Technical Report 88-07, 66 pp.
- Henkel, H. in press: Magnetic crustal structures in northern Fennoscandia. *Tectonophysics*
- Henkel, H. in Ambros, M. 1980: Description of the geological maps Lannavaara NV, NO, SV, SO and Karesuando SV, SO. *Sver. geol. unders. Af* 25-30, 57-111.
- Henkel, H. & Guzmán, M. 1977: Magnetic features of fracture zones. *Geoexploration* 15, 173-181.

- Henkel, H. & Eriksson, L. 1980: Interpretation of low altitude airborne magnetic and VLF measurements for identification of fracture zones. In: M. Bergman (ed.) *Subsurface Space*. Pergamon Press, Oxford.
- Henkel, H., Hult, K., Eriksson, L. & Johansson, L. 1983: Neotectonics in northern Sweden - geophysical investigations. *Svensk kärnbränsleförsörjning AB/Avdeling KBS Technical Report 83-57*, 64 pp.
- Henkel, H., Aaro, S., Hultström, J., Kero, L., Mellander, H. & Andersson, C. 1984: Filipstadprojektet - en test av bildebehandlingssystemet EBBA-1 för regionala geofysiske data. *SGU Geophysical Report 8408*, 93 pp.
- Hesselström, B. 1987: *GAMMA86 user's manual*. Swedish Geological Company, Uppsala, 27 pp.
- Holmsen, P., Padget, P. & Pehkonen, E. 1937: The Precambrian geology of Vest-Finnmark, Northern Norway. *Nor. geol. unders.* 201, 106 pp.
- Holst, B. 1986: Kombinert tolkning av geofysikk og geologi på kartblad 1832 I Siebe i Kautokeino-området, Finnmark. Unpubl. thesis, NTH, University of Trondheim, 109 pp.
- Håbrekke, H. 1979: Magnetiske-, elektromagnetiske-, radiometriske- og VLF-målinger fra helikopter over et område syd for Kautokeino, Finnmark. *NGU Report 1734*, 12 pp.
- Håbrekke, H. 1980a: Magnetiske-, elektromagnetiske-, VLF- og radiometriske målinger fra helikopter over Kautokeino syd, Kautokeino, Finnmark. *NGU Report 1782*, 12 pp.
- Håbrekke, H. 1980b: Magnetiske-, elektromagnetiske-, VLF- og radiometriske målinger fra helikopter over Bidjovagge-området, Kautokeino, Finnmark. *NGU Report 1783*, 12 pp.
- Håbrekke, H. 1981: Magnetiske-, elektromagnetiske-, VLF- og radiometriske målinger fra helikopter over Bidjovaggeområdet, Kautokeino, Finnmark. *NGU Report 1833*, 12 pp.
- Håbrekke, H. 1983: Geofysiske målinger fra helikopter over et område rundt Masi, Kautokeino, Finnmark. *NGU Report 1902*, 15 pp.
- Håbrekke, H. 1984: Geofysiske målinger fra helikopter over kartbladene Carajav'ri og Jiesjav'ri, Finnmark. *NGU Report 1886/8*, 15 pp.
- Ingersoll, R.V. 1988: Tectonics of sedimentary basins. *Geol. Soc. Am. Bull.* 100, 1704-1719.
- Kaikkonen, P. 1979: Numerical VLF modelling. *Geophysical Prospecting* 27, 815-834.
- Krill, A.G. 1985: Svecokarelian thrusting with thermal inversion in the Karasjok-Levajok area of the northern Baltic Shield. *Nor. geol. unders. Bull.* 403, 89-101.
- Krill, A.G., Berg, S., Lindahl, I., Mearns, E.W., Often, M. and Olerud, S., Olesen, O., Sandstad, J.S., Siedlecka, A., Solli, A. 1985: Rb-Sr, U-Pb, and Sm-Nd isotopic dates from the Precambrian rocks of Finnmark, *Nor. geol. unders. Bull.* 403, 37-54.

- Lee, M.K., Pharaoh, T.C. & Soper, N.J. 1990: Structural trends in central Britain from images of gravity and aeromagnetic fields. *Journ. Geol. Soc., London* 147, 241-258.
- Lile, O.B. & Singsaas, P. 1978: Teori om årsaken til VLF anomalier og sammenligning av VLF og Turam anomalier. Paper presented at Noftig meeting, Oulo, Finland.
- Lippard, S.J. & Roberts, D. 1987: Fault systems in Caledonian Finnmark and the southern Barents Sea. *Nor. geol. unders. Bull.* 410, 55-64.
- Lindroos, H. & Henkel, H. 1978: Regional geological and geophysical interpretation of Precambrian structures in Northeastern Sweden. *Sver. geol. unders.* C751, 19 pp.
- McKenzie, D. 1978: Some remarks on the development of sedimentary basins. *Earth and Planet. Sci. Let.* 40, 25-32.
- Michard-Vitrac, A., Albarede, F., Dupuis, C., & Taylor, H.P. 1980: The genesis of Variscan plutonic rocks - Inferences from Sr, Pb, and U studies on the Maladeta Igneous Complex, central Pyrenees, Spain. *Contr. Miner. and Petr.* 72, 57-72.
- Mertanen, S., Pesonen, L.J., & Leino, M. 1990: Uusia paleomagneettisia tuloksia Fennoskandian diabaaseista. Summary: New paleomagnetic results of diabase dykes in Fennoscandia. *Geologi* 42, 55-56.
- Mogaard, J.O. & Skilbrei, J.R. 1986: Geofysiske målinger fra helikopter over kartbladene Kautokeino, Lappaluobbal, Siebe og Addjit, Finnmark fylke. Unpubl. NGU Report 86.054, 22 pp.
- Muir Wood, R. 1989: Extraordinary deglaciation reverse faulting in northern Fennoscandia. In: S. Gregersen & P.W. Basham (eds.) *Earthquakes at North-Atlantic passive margins: neotectonics and postglacial rebound*. NATO ASI series. Series C, Mathematical and physical sciences, vol. 266. Kluwer Academic Publishers, Dordrecht, The Netherlands, 141-173.
- Norges geografiske oppmåling 1979a: Gravity anomaly map, terrain-corrected Bouguer anomalies, Nordreisa 1:250,000.
- Norges geografiske oppmåling 1979b: Gravity anomaly map, terrain-corrected Bouguer anomalies, Enontekiö 1:250,000.
- Norges geologiske undersøkelse 1981a: Aeromagnetisk kart 1933- 1:100,000. Trondheim.
- Norges geologiske undersøkelse 1981b: Aeromagnetisk kart 1832- 1:100,000. Trondheim.
- Norges geologiske undersøkelse 1981c: Aeromagnetisk kart 1833- 1:100,000. Trondheim.
- Norges geologiske undersøkelse 1981d: Aeromagnetisk kart 1932- 1:100,000. Trondheim.
- Olerud, S. 1988: Davidite-loveringite in Early Proterozoic albite felsite in Finnmark, North Norway.

- Min. Mag. 52, 400-402.
- Olesen, O. 1985: Sen-/post-glaciale forkastninger ved Masi, Finnmark. NGU Report 84.171, 27 pp.
- Olesen, O. 1988a: Petrofysiske undersøkelser, Finnmark. NGU Report 88.222, 154 pp.
- Olesen, O. 1988b: The Stuoragurra Fault, evidence of neotectonics in the Precambrian of Finnmark, northern Norway. *Nor. Geol. Tidsskr.* 68, 107-118.
- Olesen, O. & Solli, A. 1985: Geophysical and geological interpretation of regional structures within the Precambrian Kautokeino Greenstone Belt, Finnmark, North Norway. *Nor. geol. unders. Bull.* 403, 119-129.
- Olesen, O., Roberts, D., Henkel, H., Lile, O.B. & Torsvik, T. H. 1990a: Aeromagnetic and gravimetric interpretation of regional structural features in the Caledonides of West Finnmark and North Troms, northern Norway. *Nor. geol. unders. Bull.* 419, 1-24.
- Olesen, O., Henkel, H., Lile, O.B., Muring, E. & Rønning J.S. 1990b: Detailed geophysical investigations of the Stuoragurra postglacial fault, Finnmark, northern Norway. NGU Report 90.160. 42 pp.
- Olsen, K.I. in press: Beskrivelse til de berggrunnsgeologiske kart: Kautokeino 1833 I, Adjitt 1832 IV, Siebe 1832 I, Urdutoai'vi 132 III, Roavvoaivi 1832 II M 1:50.000, Finnmark. NGU Report.
- Olsen, K.I. & Nilsen, K.I. 1985: Geology of the southern part of the Kautokeino Greenstone Belt: Rb-Sr geochronology and geochemistry of associated gneisses and late intrusions. *Nor. geol. unders. Bull.* 403, 131-160.
- Sandstad, J.S. 1983: Berggrunnsgeologisk kartlegging av prekambrisk grunnfjell innen kartbladet Mållejus, Kvænangen/Kautokeino, Troms/Finnmark. NGU Report 1886/5, 28 pp.
- Sandstad, J.S. 1985: Mållejus. Foreløbig berggrunnsgeologisk kart 1833 IV - 1:50 000. *Nor. geol. unders.*
- Siedlecka, A. 1985: Geology of the Iesjav'ri - Skoganvarre area, Northern Finnmarksvidda, North Norway. *Norges geologiske undersøkelse* 403, 103-112.
- Siedlecka, A., Iversen, E., Krill, A. G., Lieungh, B., Often, M., Sandstad, J. S. & Solli, A. 1985: Lithostratigraphy and correlation of the Archean and early Proterozoic rocks of Finnmarksvidda and the Sørvaranger district. *Norges geol. unders. Bull.* 403, 7-36.
- Skilbrei, J.R. 1986: Magnetisk residualfeltkart, Finnmarksvidda, M 1:250.000. NGU Report 86.158, 13 pp.
- Solli, A. 1983: Precambrian stratigraphy in the Masi area, Southwestern Finnmark, Norway. *Nor. geol. unders.* 380, 97-105.

- Solli, A. 1988: Masi, 1933 IV - berggrunnsgeologisk kart - M 1:50 000. Nor. geol. unders., Trondheim.
- Solli, A. 1990: Carajav'ri, 1833 I - berggrunnsgeologisk kart - M 1:50 000. Nor. geol. unders., Trondheim.
- Swain, C.J. 1976: A Fortran IV program for interpolating irregularly spaced data using the difference equations for minimum curvature. *Computers & Geosciences* 1, 231-240.
- Sylvester, A.G. 1988: Strike-slip faults. *Geol. Soc. of Am. Bull.* 100, 1666-1703.
- Sylvester, A.G. & Smith, R.R. 1976: Tectonic transpression and basement-controlled deformation in the San Andreas fault zone, Salton Trough, California. *American Association of Petroleum Geologists Bulletin* 60, 2081-2102.
- Talbot, C. 1986: A preliminary structural analysis of the pattern of post-glacial faults in northern Sweden. Svensk kärnbränsleförsörjning AB/Avdeling KBS Unpublished Technical Report 86.20, 36 pp.
- Tapponier, P., Peltzer, G. & Armijo, R. 1986: On the mechanics of the collision between India and Asia. In Covard, M.P. & Reis, A.C. (eds.) *Collision tectonics*. *Geol. Soc. London Spec. Publ.* 19, 115-157.
- Townsend, C., Rice, A.H.N. & Mackay, A. 1989: The structure and stratigraphy of the southwestern portion of the Gaissa Thrust Belt and the adjacent Kalak Nappe Complex, Finnmark, N Norway. In: Gayer, R.A. (ed.) *The Caledonide Geology of Scandinavia*. Graham & Trotman, London, 111-126.
- Vik, E. 1981: Bergmark gruvefelt, Kvænangen, Troms. Foreløpig rapport fra geologiske og geofysiske undersøkelser 1979-1980. Unpubl. NGU Report 1800/46C, 50 pp.
- Watterson, J. 1978: Proterozoic intraplate deformation in the light of southeast Asian neotectonics. *Nature* 273, 636-640.
- Wilcox, R.E., Harding, T.P. & Seely, D.R. 1973: Basic wrench tectonics: *Am. Ass. of Petr. Geol. Bull.* 57, 74-96.
- Woodcock, N.H. & Fischer, M. 1986: Strike-slip duplexes. *Journ. Struct. Geol.* 8, 725-735.
- Zwaan, K.B. & Gautier, A.M. 1980: Alta og Gargia. Beskrivelse til de berggrunnsgeologiske kart 1834 I og 1934 IV, M 1:50.000. *Nor. geol. unders* 357, 1-47.
- Zwaan, K.B. 1988: Nordreisa, berggrunnsgeologisk kart - M 1:250 000. *Nor. geol. unders.*, Trondheim.

## LIST OF FIGURES

Fig. 1. Simplified bedrock geology map of western Finnmarksvidda; part of the 1:1 million bedrock geological map of northern Fennoscandia (Geological Surveys of Finland, Norway and Sweden 1987). JeC - Jer'gul Gneiss Complex; RaC Rai'sædno Gneiss Complex; GåF - Gåldenvarri Formation; VuF - Vuomegielas Formation; MsF - Masi Formation; CsF - Cas'kejas Formation; SuF - Suoluvuobmi Formation; LiF - Lik'ca Formation; BiF - Bik'kacákka Formation; CaF - Caravarri Formation; DiG - Dividal Group.

Fig. 2. Susceptibility spectra of in situ measurements on amphibolite and greenschist-facies tuffite, metadiabase and metasediments within the Cas'kejas Formation.

Fig. 3. Susceptibility spectra of in situ measurements on albite diabase in the Masi area. Logarithmic mean values (m) and standard deviations (s) expressed in decades are given in SI units.

Fig. 4. Plots of natural remanent magnetization (NRM) directions of (A) diabase and (B) albite diabase on a Wulff net (lower hemisphere). Filled and open circles show positive and negative inclination, respectively. Plot (A) of the albite diabase shows a smeared distribution. It is concluded that this remanence to a great extent is viscous. Plot (B) shows a more condensed distribution. One outlier in (B) is ignored in the calculation of the statistics.

Fig. 5. Shaded relief image of the low-altitude measurements from the Kautokeino Greenstone Belt.

Fig. 6. Shaded relief image of the digital topography from the Kautokeino Greenstone Belt.

Fig. 7. Gravity section across the Kautokeino Greenstone Belt. Location of the profile shown in Plate 2. A section of the profile is crossing the map area in Fig. 11.

Fig. 8. Aeromagnetic map and tectonic interpretation, Masi area.

Fig. 9. Gravity map and tectonic interpretation, Masi area.

Fig. 10. Digital topography and tectonic interpretation, Masi area.

Fig. 11. Tectonic interpretation map, Masi area. A section of gravity profile ABC is indicated on the map.

Fig. 12. (2 pages) Aeromagnetic interpretation profiles. Location of the profiles shown in Fig. 11. Bodies which are poorly constrained from the magnetic data are shown with dashed lines.

Fig. 13. A three-dimensional perspective model of the Masi area generated with the Erdas 3D module (Erdas 1990b). The vertical scale is exaggerated by a factor of 2. The view is towards the southwest along the MSFZ. The Biggevarri Duplex can be seen in the middle of the picture to the south of Masi. The shaded area at the southern margin of the duplex structure has been investigated in detail by Olesen et al. (1990b).

Fig. 14. Sketch map of regional structural elements interpreted from aeromagnetic and gravity data in Finnmark and adjacent areas in northern Finland and northern Sweden (Modified from Geological Surveys of Finland, Norway and Sweden 1986b, Midtun 1988, Olesen et al. 1990a, Henkel in press). BKFC - Bothnian-Kvænangen Fault Complex; KAFZ - Karesuando-Arjeplog Fault Zone; MSFZ - Mierujav'ri-Sværholt Fault Zone; LVFZ - Langfjord-Vargsund Fault Zone.

## LIST OF PLATES

Plate 1. Aeromagnetic map, Kautokeino Greenstone Belt.

Plate 2. Residual gravity map, Kautokeino Greenstone Belt.

Plate 3. Digital topography, Kautokeino Greenstone Belt.

Plate 4. Geophysical interpretation map superimposed on digital topography, Kautokeino Greenstone Belt. Major fault zones interpreted from the geophysical images. MSFZ - Mierujav'ri-Sværholt Fault Zone; CBL - Ciednjaljåkka-Boaganjav'ri Lineament; SBF - Soadnujav'ri-Bajasjav'ri Fault.



## TABLES

Table 1. Rock densities applied in the gravity modelling, Kautokeino Greenstone Belt. Extended tables are given in Olesen & Solli (1985) and Olesen (1988a).

Rock unit	No.	Density Mean	(10 <sup>3</sup> kg/m <sup>3</sup> ) st.dev.
Rai'sædno Gneiss Complex	86	2.69	.14
Jer'gul Gneiss Complex	457	2.69	.11
Gål'denvarri Formation	80	2.96	.11
Masi Formation	117	2.65	.07
Cas'kejas Formation (Amphibolite facies)	198	2.96	.10
Cas'kejas Formation (Greenschist facies)	65	2.88	.12
Suoluvuobmi Formation Metavolcanics	144	2.97	.10
Suoluvuobmi Formation Metasediments	72	2.73	.06
Lik'ca Formation	182	2.85	.19
Caravarri Formation	52	2.66	.06
Albite diabase	55	2.91	.10

Table 2. Statistical data; density, susceptibility and Q-value for albite diabases in the Masi area and in Karesuando-Lannavaara, northern Sweden (Henkel 1980). Units are in SI. The standard deviation of the magnetic properties is expressed in decades. Magnetic properties have logarithmic mean values.

	Masi area			Lannavaara and Karesuando (Henkel 1980)	
	n=55 mean	st.dev.		n=27 mean	st.dev.
Density ( $10^3$ kg/m <sup>3</sup> )	2.91	.10		2.94	.08
Susceptibility	.07	.50		.13	.80
Q-value	.28	.23	n=11	.46	.44
NRM declination	207°			45°	
inclination	69°			75°	

## APPENDIX, page 1

VLF ground profiles across the MSFZ. The locations of the profiles are shown in Figs. 8, 9, 10 & 11. Arrows indicate the intersections with the SF. Steep negative gradients of the real component show locations of electrical conductors interpreted as water-containing faults.

### Legend

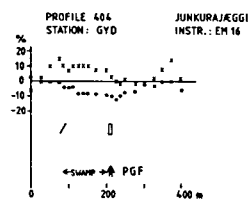
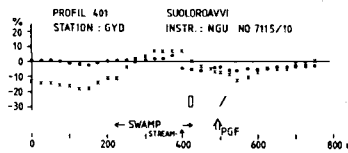
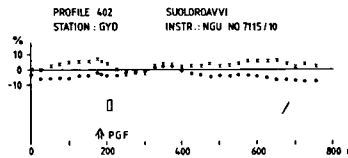
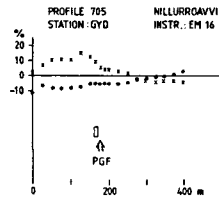
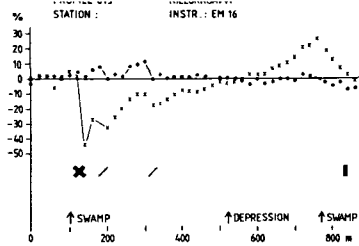
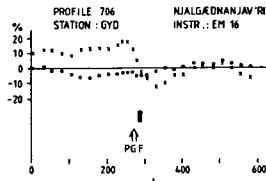
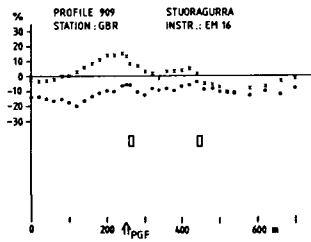
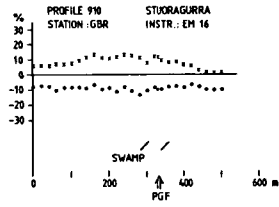
- × Real component
- Imaginary "

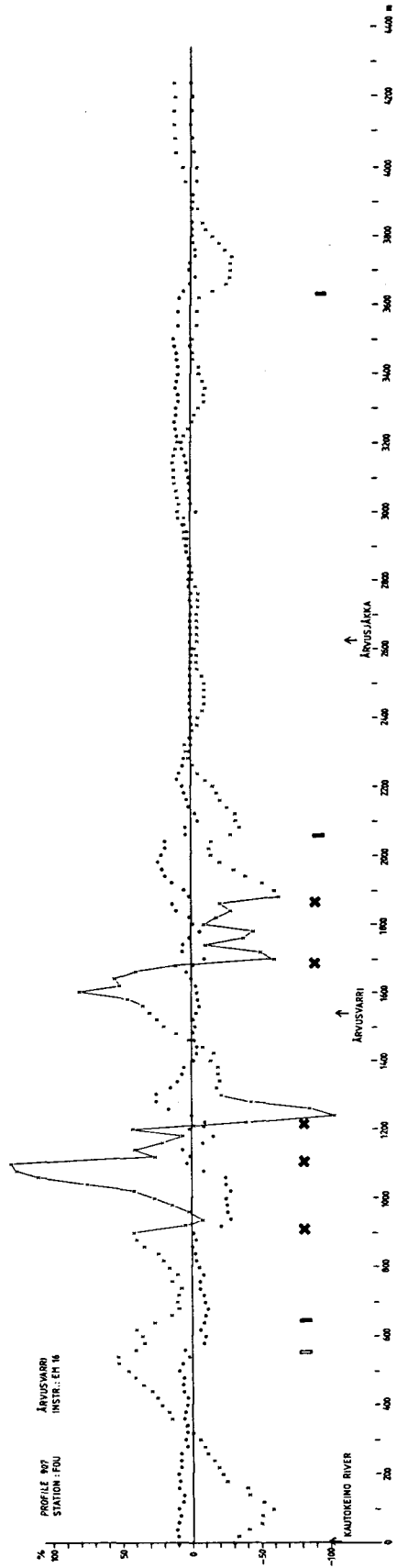
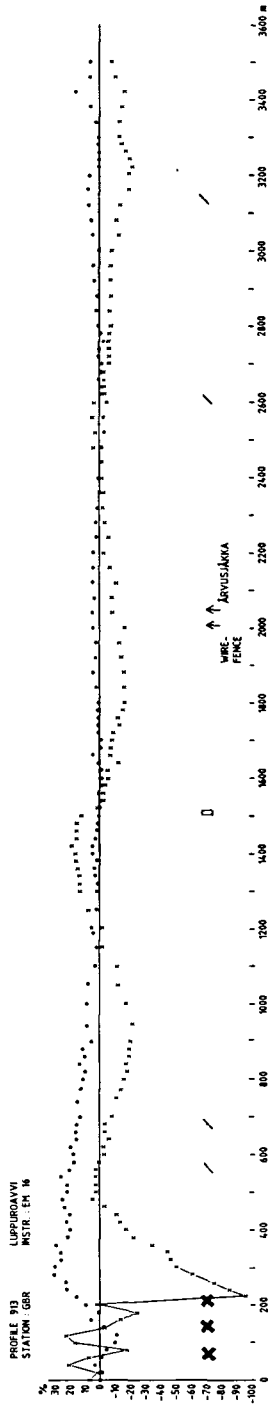
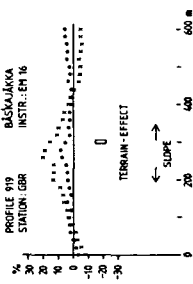
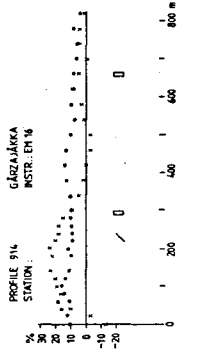
Classification of the real component anomalies (peak to peak), A

- / 5% < A < 10%
- ▣ 10% < A < 20%
- 20% < A < 40%
- × 40% < A

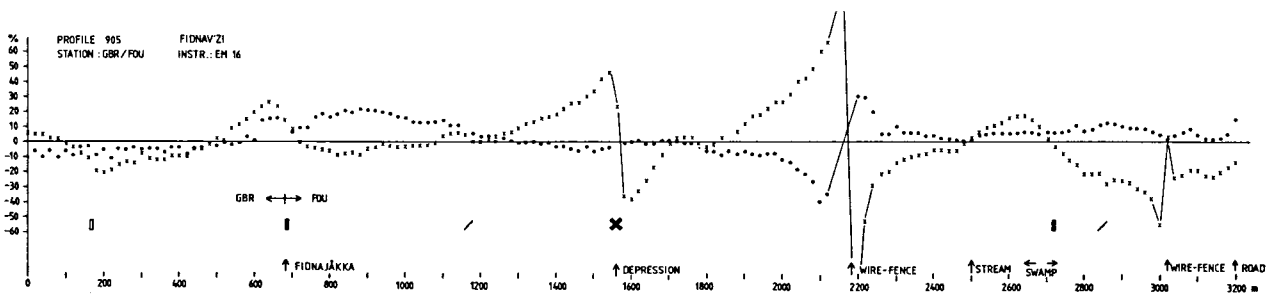
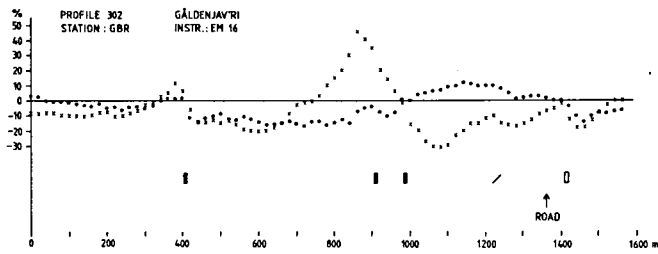
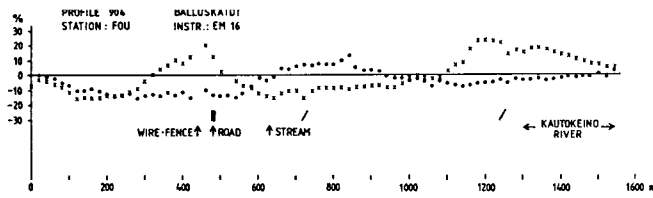
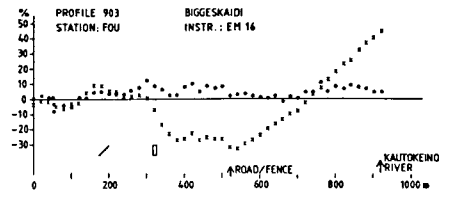
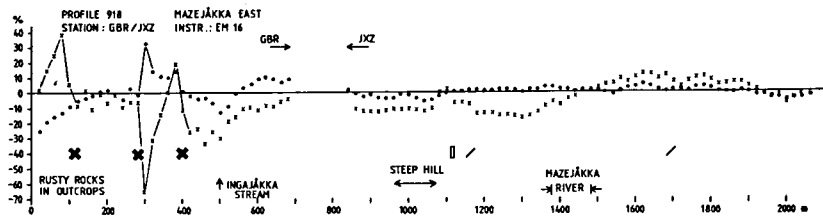
PGF Postglacial fault

Appendix, page 2

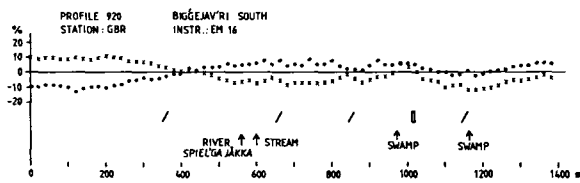
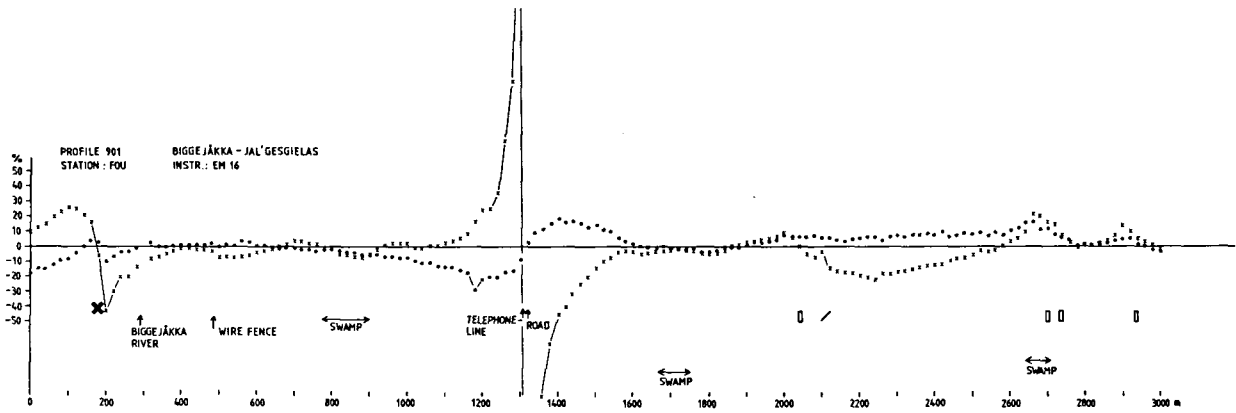
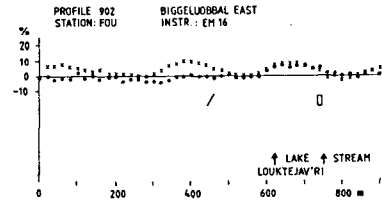
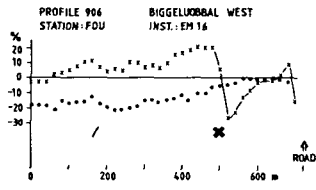
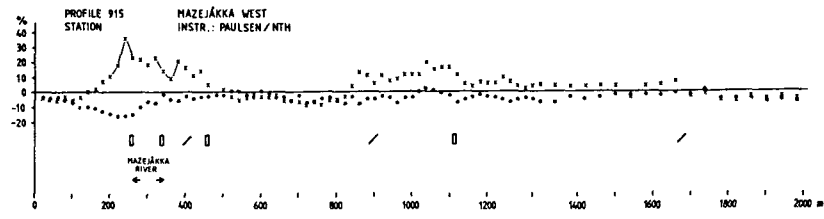


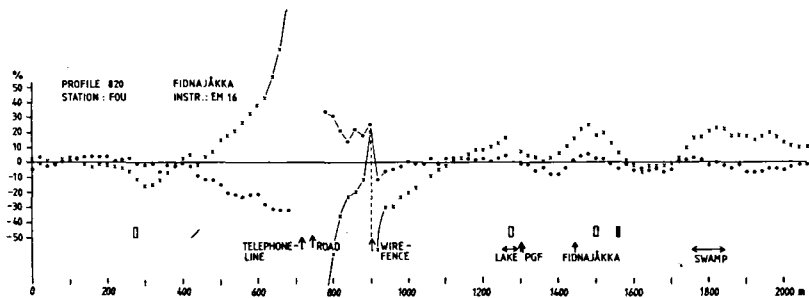
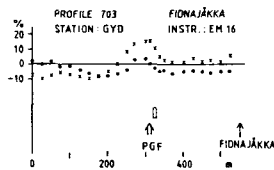
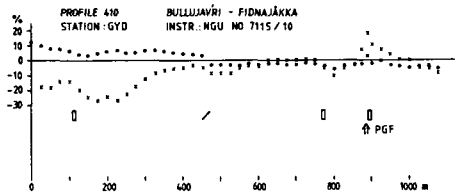
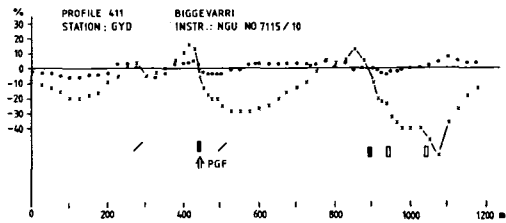
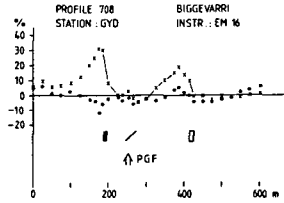
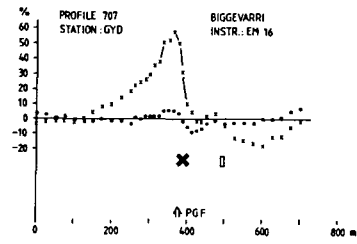


# Appendix, page 4



# Appendix, page 5







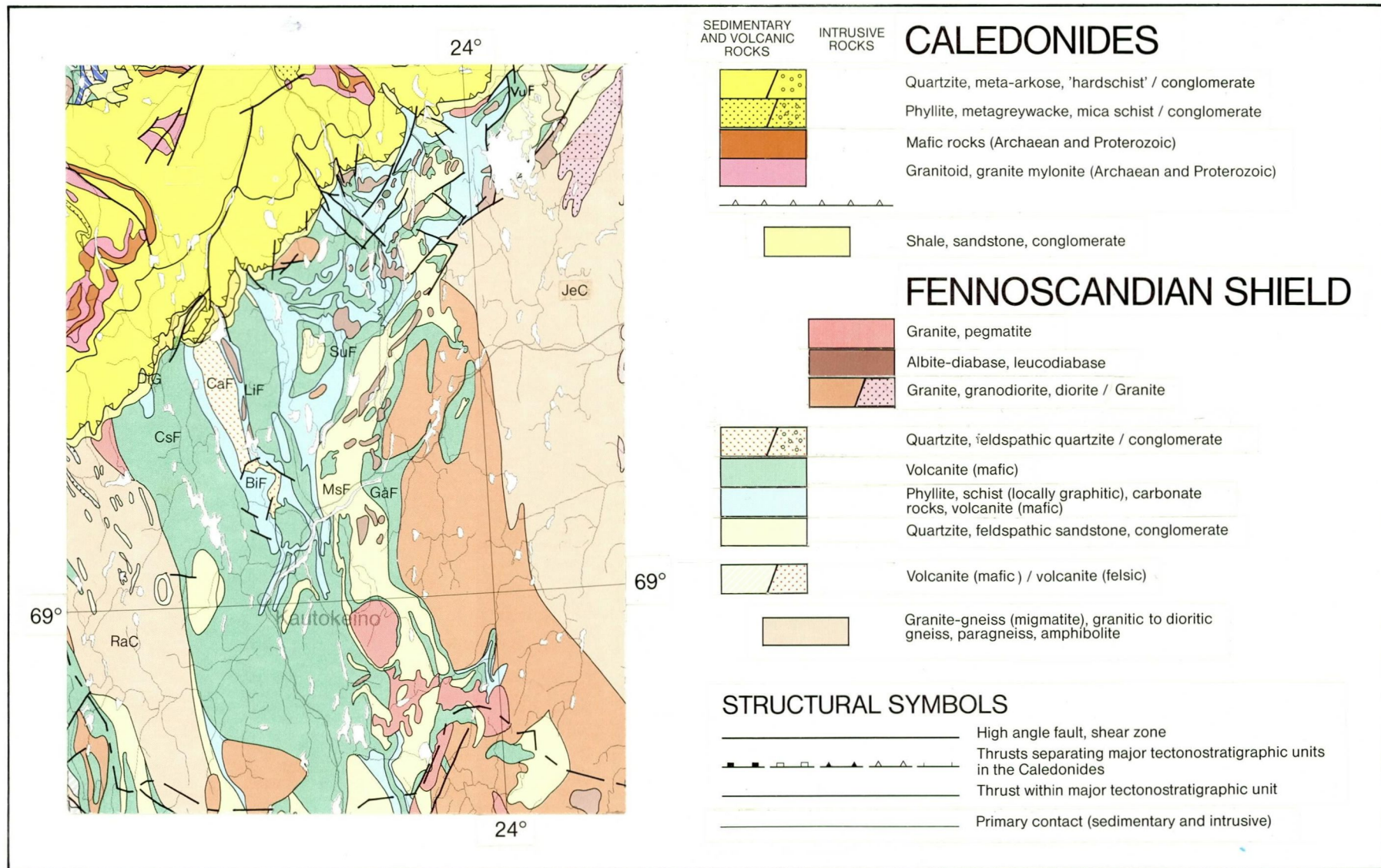
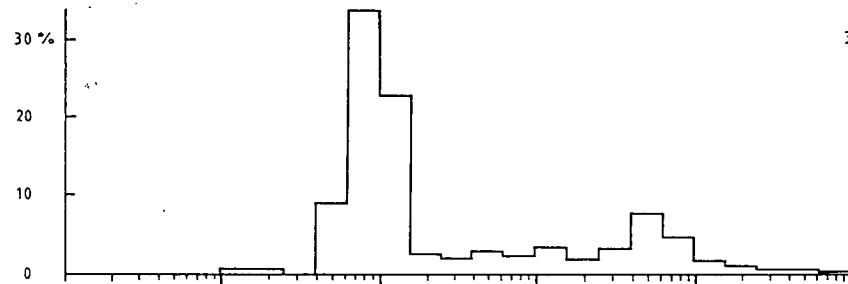


Fig. 1. Simplified bedrock geology map of western Finnmarksvidda; part of the 1:1 million bedrock geological map of northern Fennoscandia (Geological Surveys of Finland, Norway and Sweden 1987). JeC - Jer'gul Gneiss Complex; RaC Rai'sædno Gneiss Complex; GåF - Gåldenvarri Formation; VuF - Vuomegielas Formation; MsF - Masi Formation; CsF - Cas'kejas Formation; SuF - Suoluvuobmi Formation; LiF - Lik'ca Formation; BiF - Bik'kacåkka Formation; CaF - Caravarri Formation; DiG - Dividal Group.

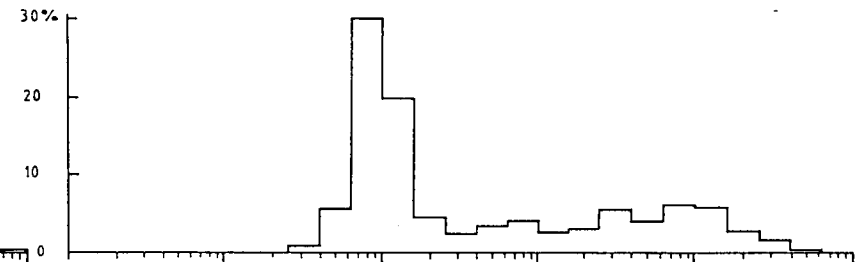
ČASKE'JAS FORMATION WEST  
AMPHIBOLITE FACIES

TUFFITE  
n = 203

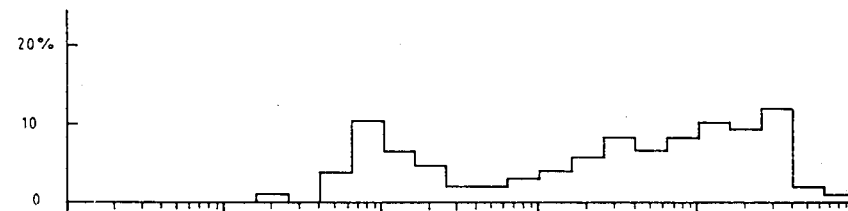


ČASKE'JAS FORMATION EAST  
GREENSCHIST FACIES

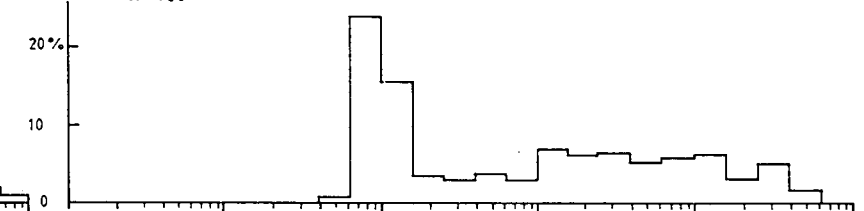
TUFFITE  
n = 396



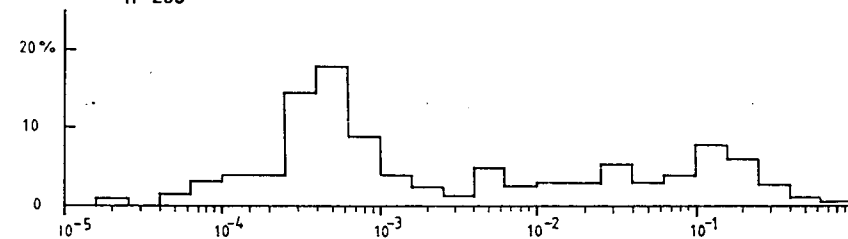
METADIABASE  
n = 108



METADIABASE  
n = 400



ARGILLITE  
n = 268



METASEDIMENTS  
n = 36

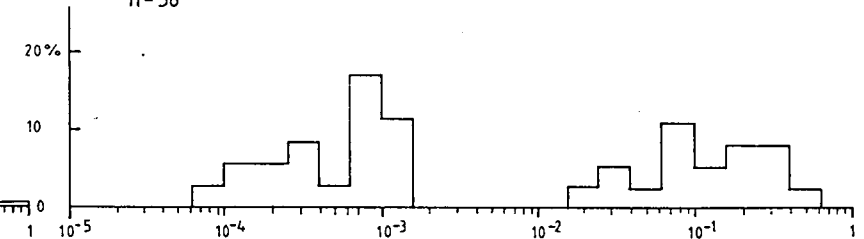


Fig. 2. Susceptibility spectra of in situ measurements on amphibolite and greenschist-facies tuffite, metadiabase and metasediments within the Čas'kejas Formation.

MASI

ALBITE DIABASE

n = 161 m = 0,073 S = 0,49

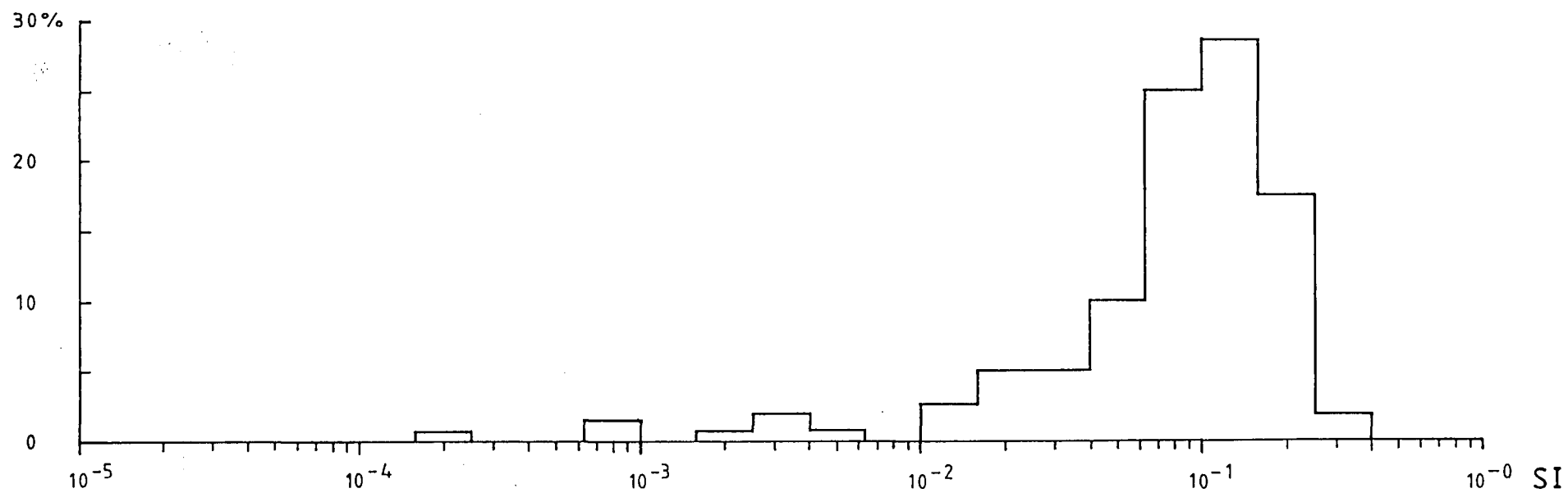


Fig. 3. Susceptibility spectra of in situ measurements on albite diabase in the Masi area. Logarithmic mean value (m) and standard deviation (s) expressed in decades are given in SI units.

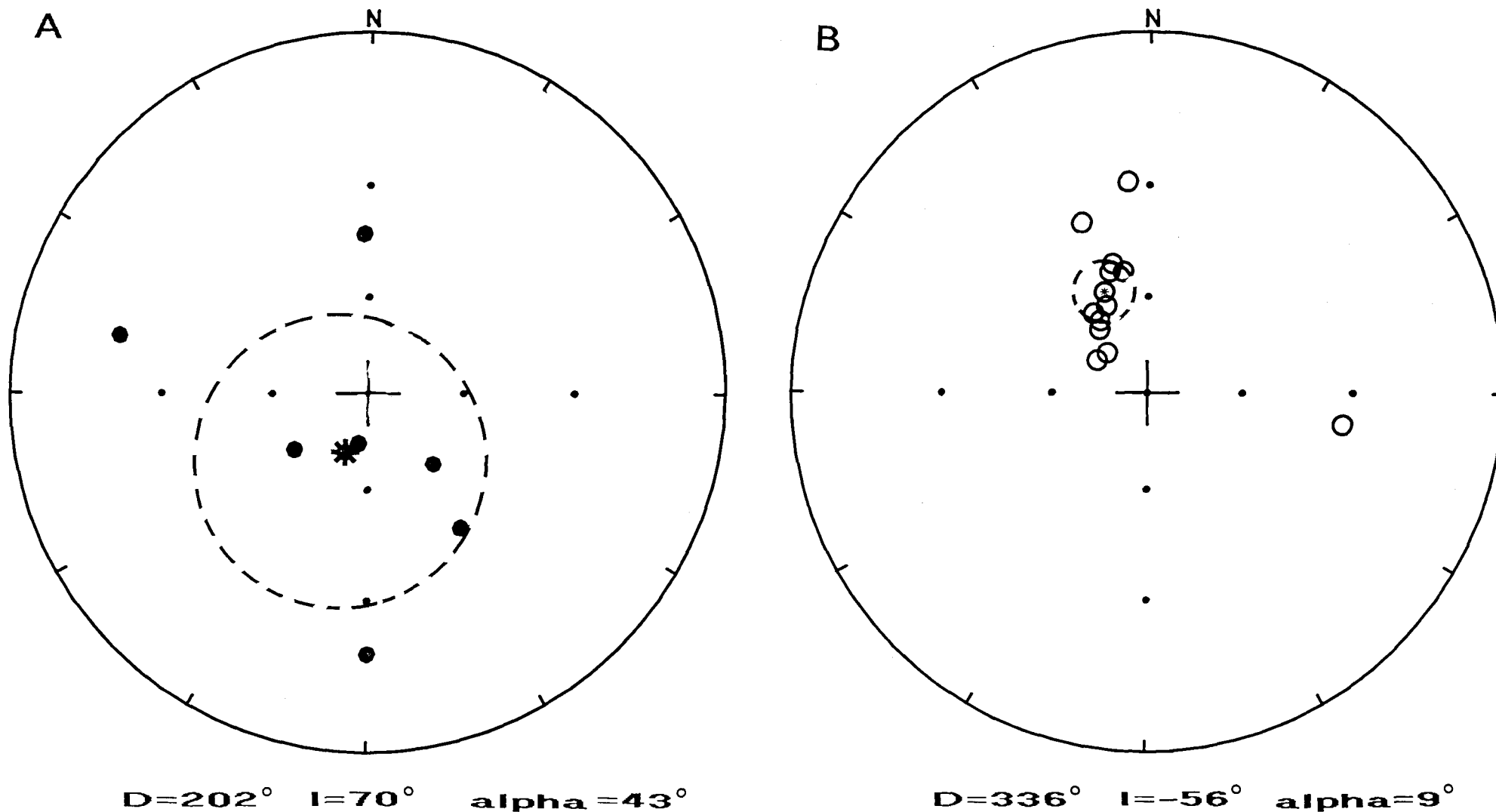


Fig. 4. Plots of natural remanent magnetization (NRM) directions of (A) albite diabase and (B) diabase on a Wulff net (lower hemisphere). Filled and open circles show positive and negative inclination, respectively. Dashed lines display the cones of 95 per cent confidence ( $\alpha$ ). Plot (A) of the albite diabase shows a smeared distribution. It is concluded that this remanence to a great extent is viscous. Plot (B) shows a more condensed distribution. One outlier in (B) is ignored in the calculation of the statistics.

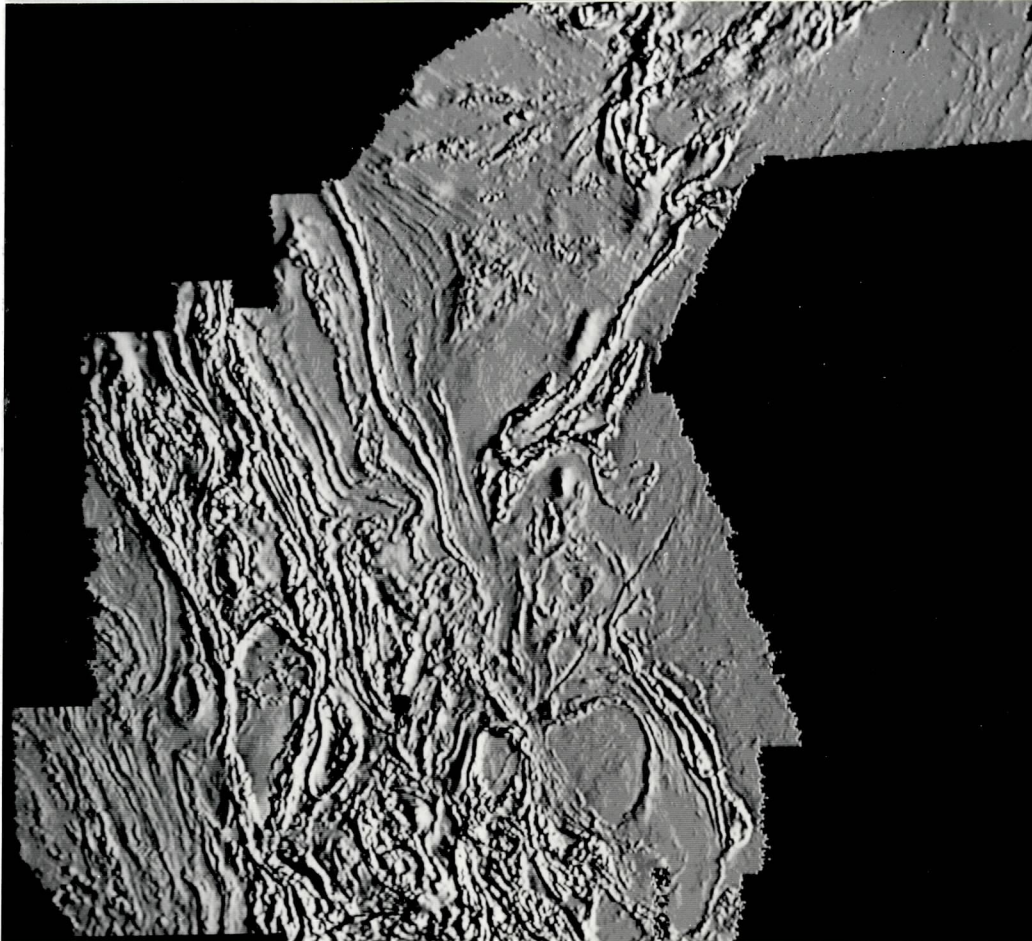


Fig. 5. Shaded relief image of the low-altitude measurements from the Kautokeino Greenstone Belt ('illumination' from the east and a 'sun inclination' of  $45^\circ$ ). For scale and location of the image; see Plate 1.



Fig. 6. Shaded relief image of the digital topography from the Kautokeino Greenstone Belt ('illumination' from the east and a 'sun inclination' of  $45^{\circ}$ ). For scale and location of the image; see Plate 3.

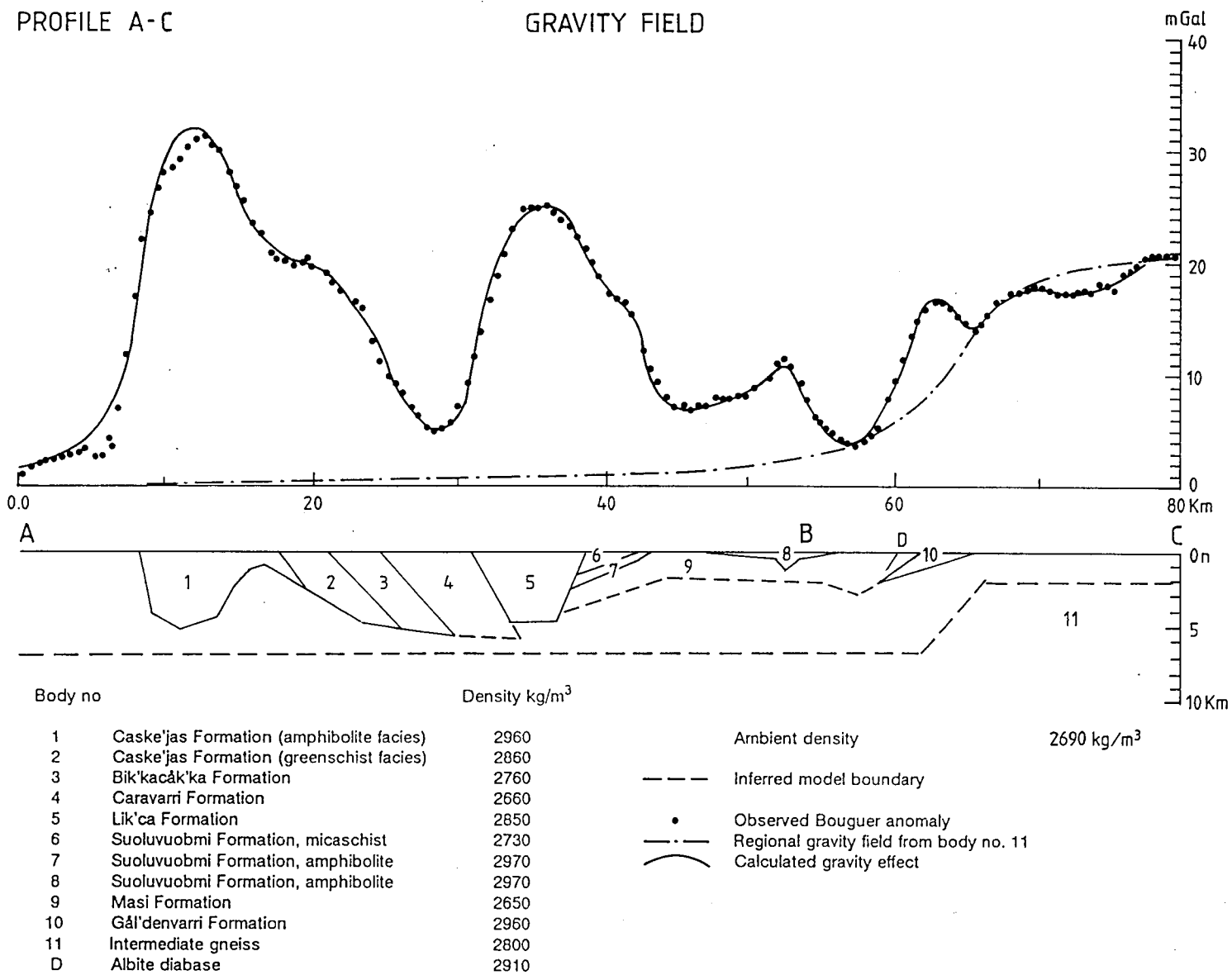


Fig. 7. Gravity section across the Kautokeino Greenstone Belt. Location of the profile shown in Plate 2. A section of the profile is crossing the map area in Fig. 11.

**Fig. 8.**

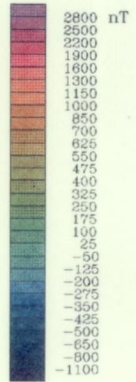
AEROMAGNETIC  
INTERPRETATION MAP  
AND  
AEROMAGNETIC  
ANOMALY MAP  
SHADED RELIEF  
TOTAL INTENSITY  
REFERRED TO DGRF-65  
FINNMARKSVIDDA  
MASI AREA



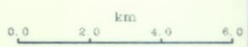
**LEGEND**

AEROMAGNETICALLY  
INDICATED FAULTS

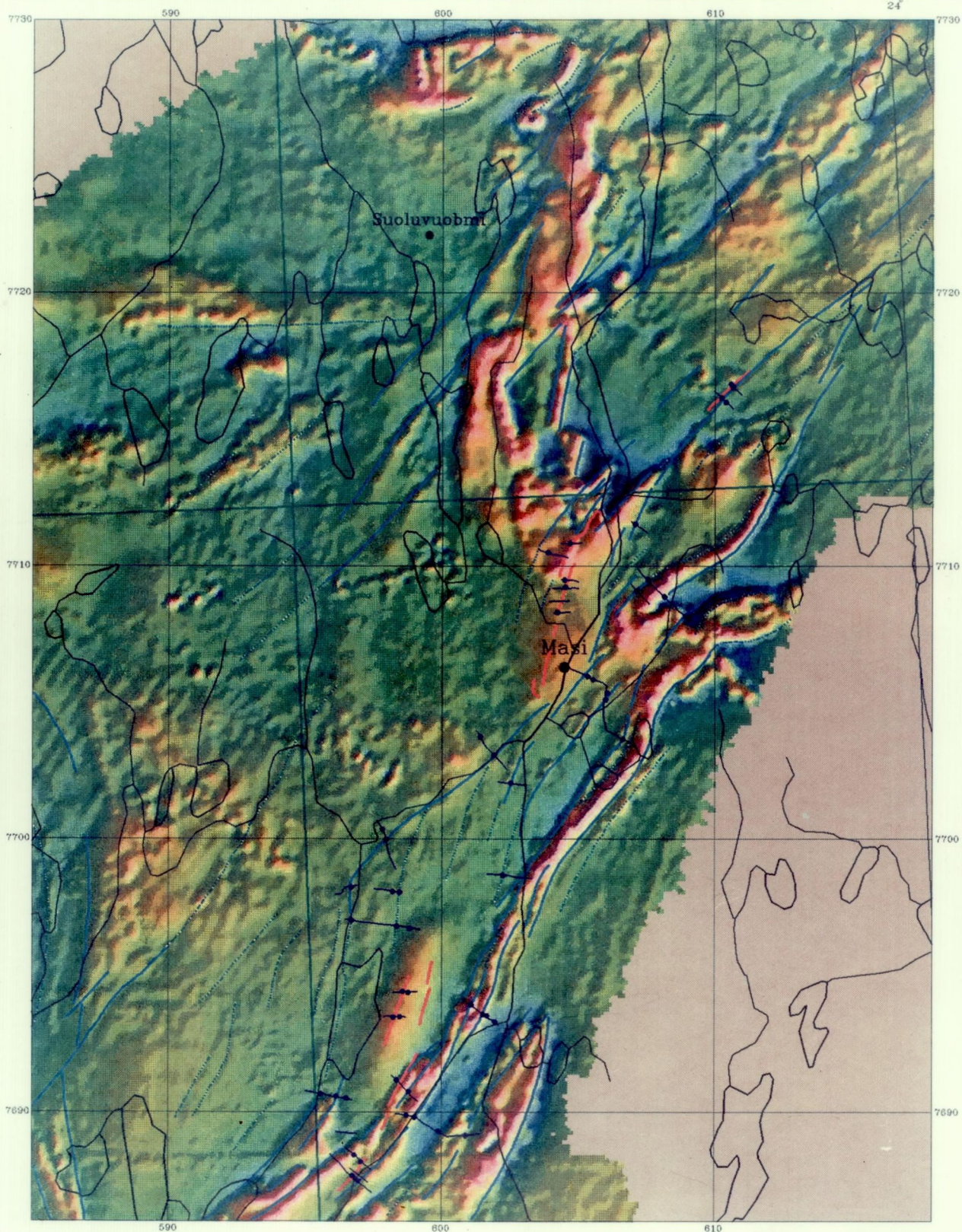
- Distinct
- Less distinct
- VLF-profile
- VLF ground truth
- Postglacial fault



UTM-ZONE 34



NGU 1990  
GEOLOGICAL SURVEY OF NORWAY






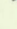



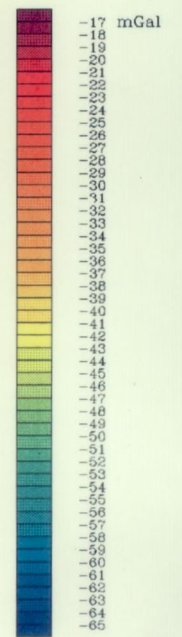
**Fig. 9.**

AEROMAGNETIC  
INTERPRETATION MAP  
AND  
BOUGUER GRAVITY  
ANOMALY MAP  
FINNMARKSVIDDA  
MASI AREA  
grid 500 x 500 m  
I.G.S.N.71 SYSTEM

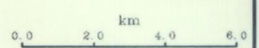
**LEGEND**

AEROMAGNETICALLY  
INDICATED FAULTS

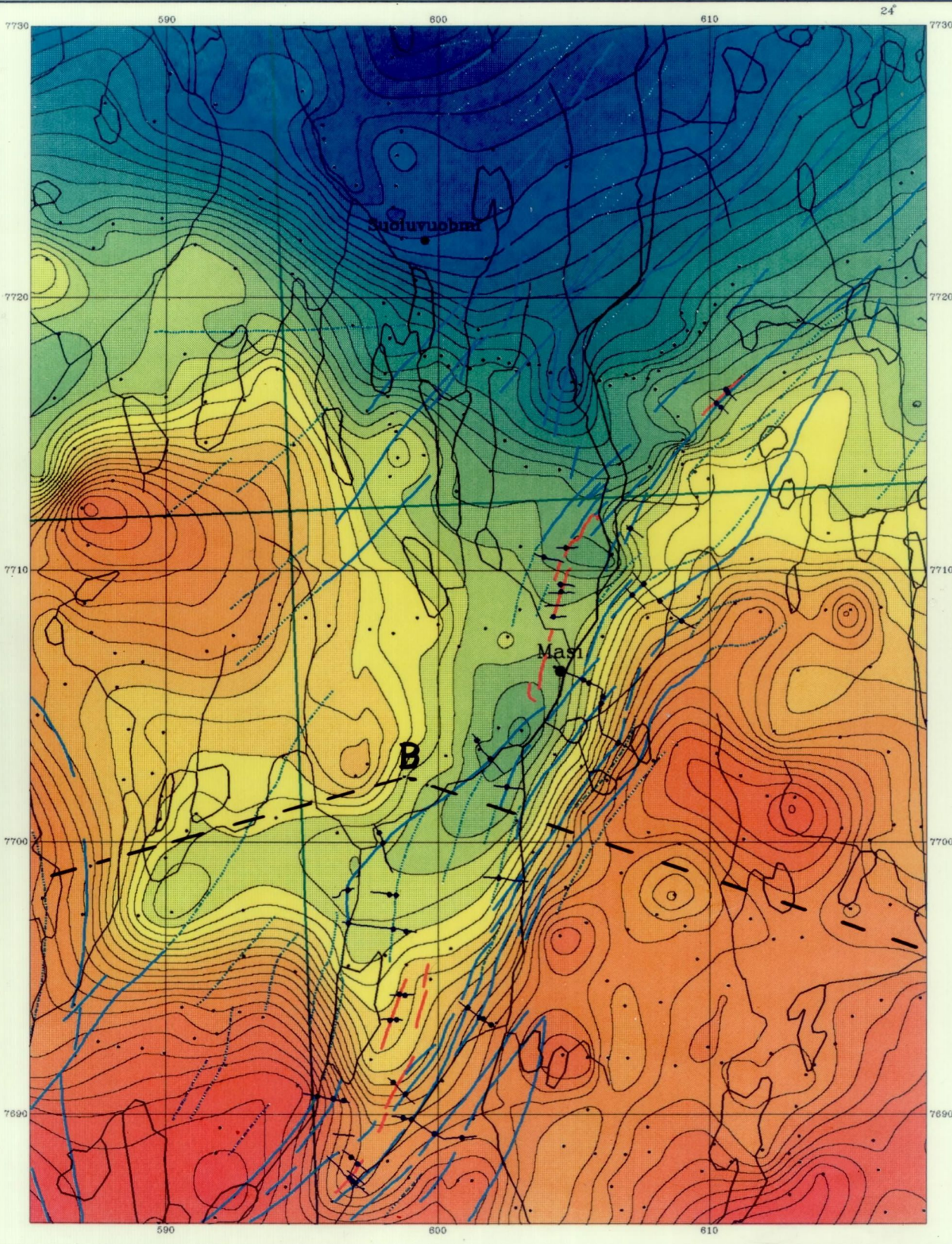
-  Distinct
-  Less distinct
-  VLF-profile
-  VLF ground truth
-  Postglacial fault



UTM-ZONE 34



NGU 1990  
GEOLOGICAL SURVEY OF NORWAY



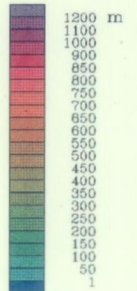
**Fig. 10.**

TOPOGRAPHY  
SHADED RELIEF  
AND  
AEROMAGNETIC  
INTERPRETATION MAP  
FINNMARKSVIDDA  
MASI AREA

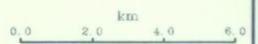


**LEGEND**

- AEROMAGNETICALLY  
INDICATED FAULTS
- Distinct
  - Less distinct
  - VLF-profile
  - VLF ground truth
  - Postglacial fault



UTM-SONE 34



NGU 1990  
GEOLOGICAL SURVEY OF NORWAY



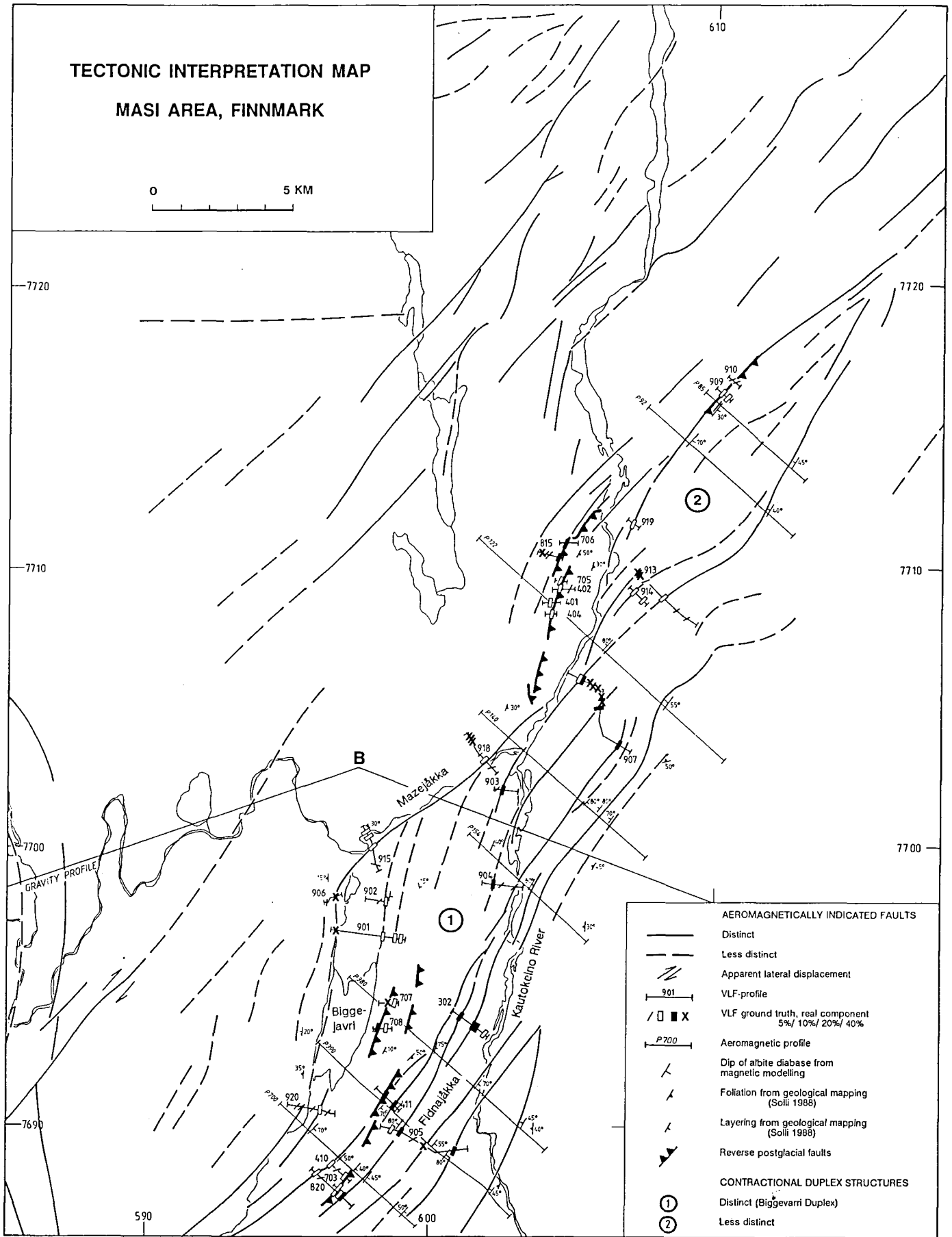


Fig. 11. Tectonic interpretation map, Masi area.

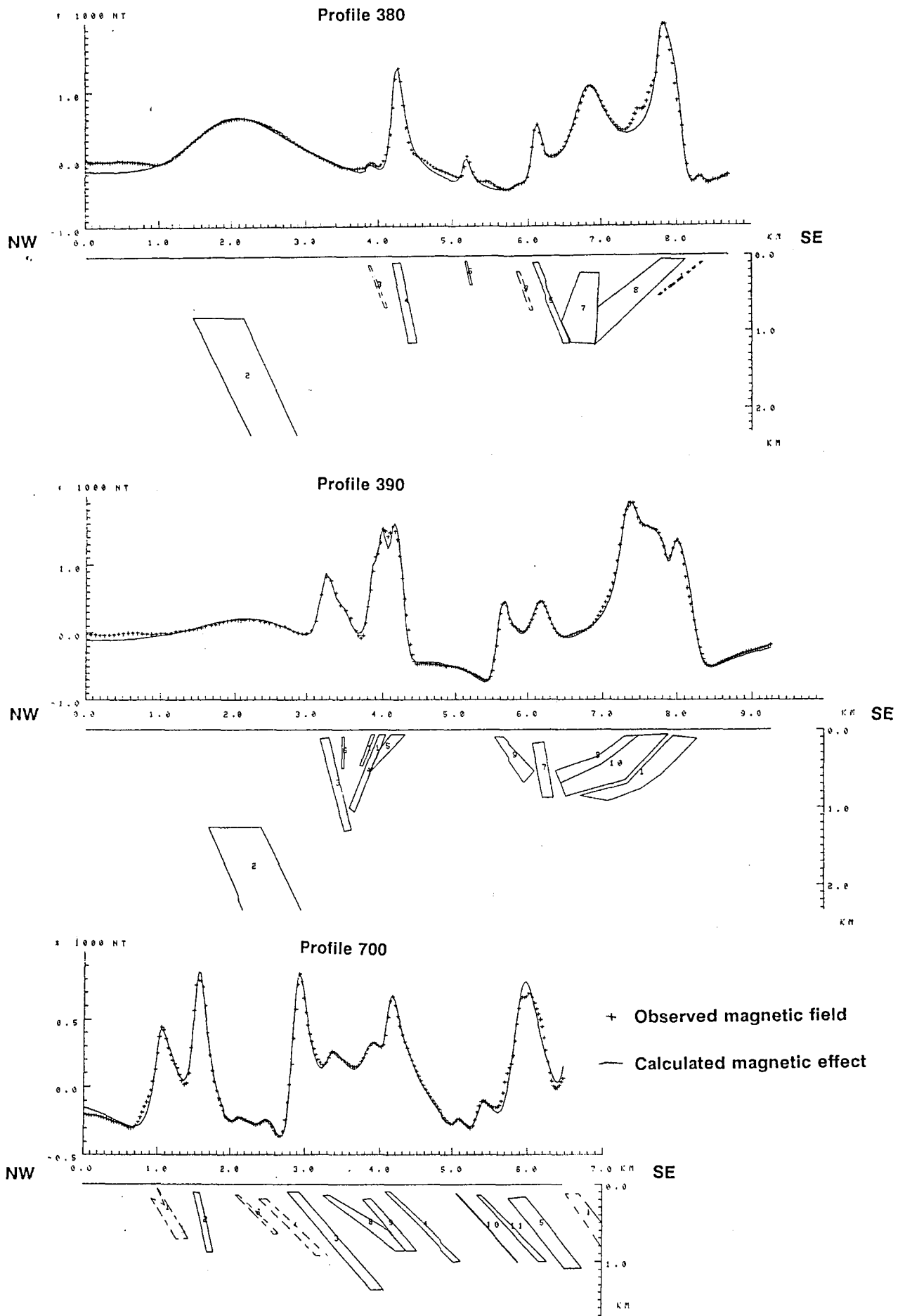


Fig. 12. Aeromagnetic modelling of albite diabases along helicopter profiles in the Masi area. Location of the profiles shown in Fig. 11. Bodies which are poorly constrained from the magnetic data are shown with dashed lines.  
 (continued over)

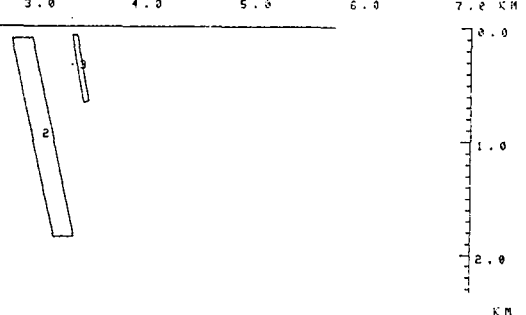
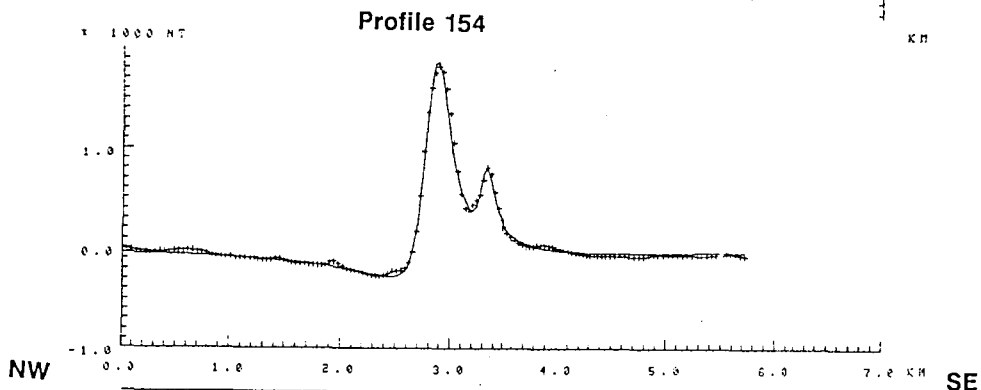
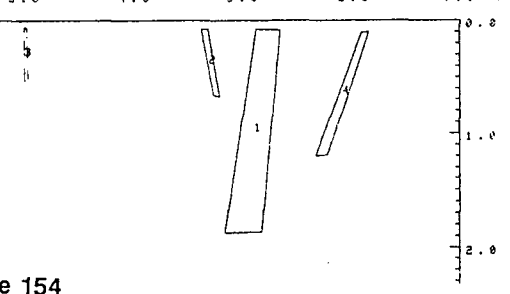
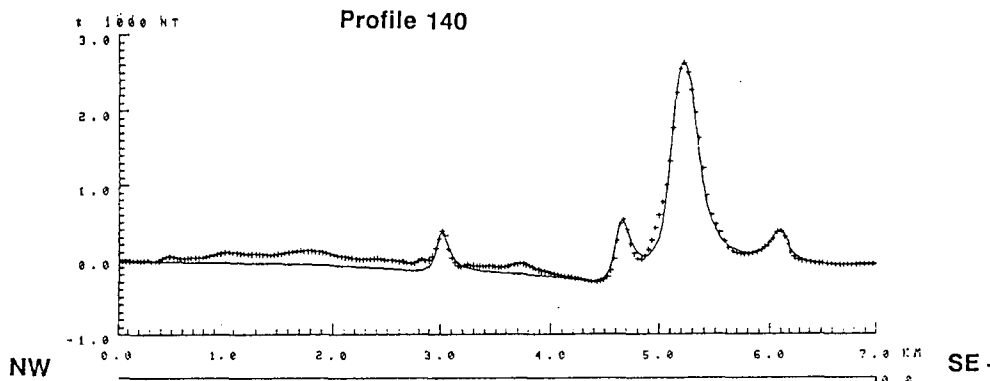
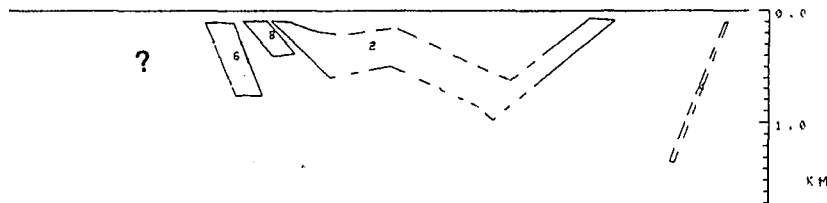
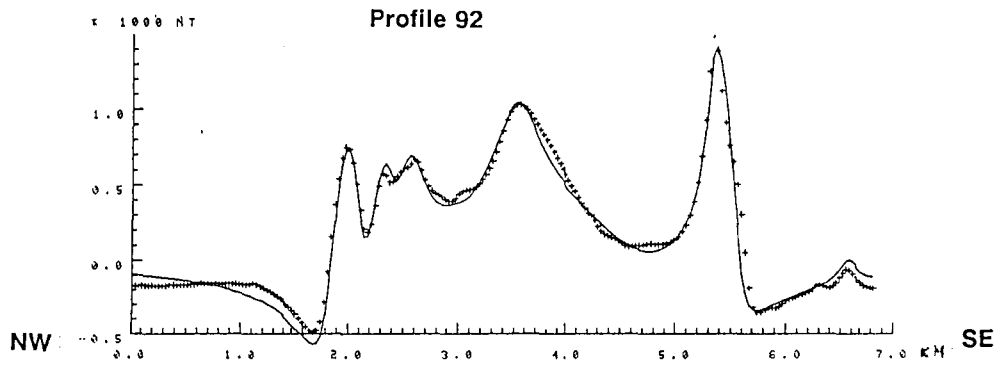


Fig. 12. continued

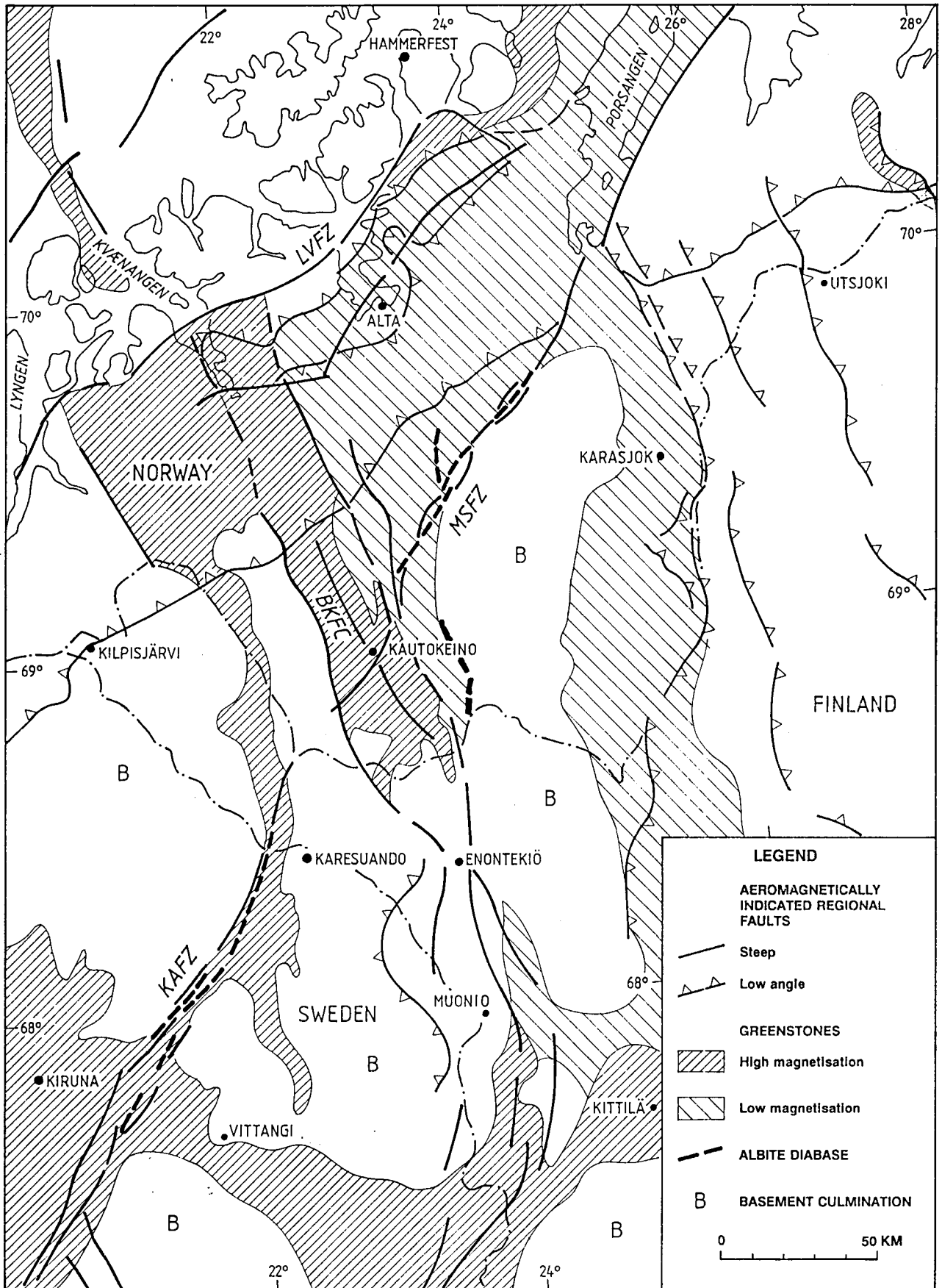


Fig. 14. Sketch map of regional structural elements interpreted from aeromagnetic and gravity data in Finnmark and adjacent areas in northern Finland and northern Sweden (Modified from Geological Surveys of Finland, Norway and Sweden 1986b, Midtun 1988, Olesen et al. 1990a, Henkel in press). BKFC - Bothnian-Kvænangen Fault Complex; KAFZ - Karesuando-Arjeplog Fault Zone; MSFZ - Mierujav'ri-Sværholt Fault Zone; LVFZ - Langfjord-Vargsund Fault Zone.

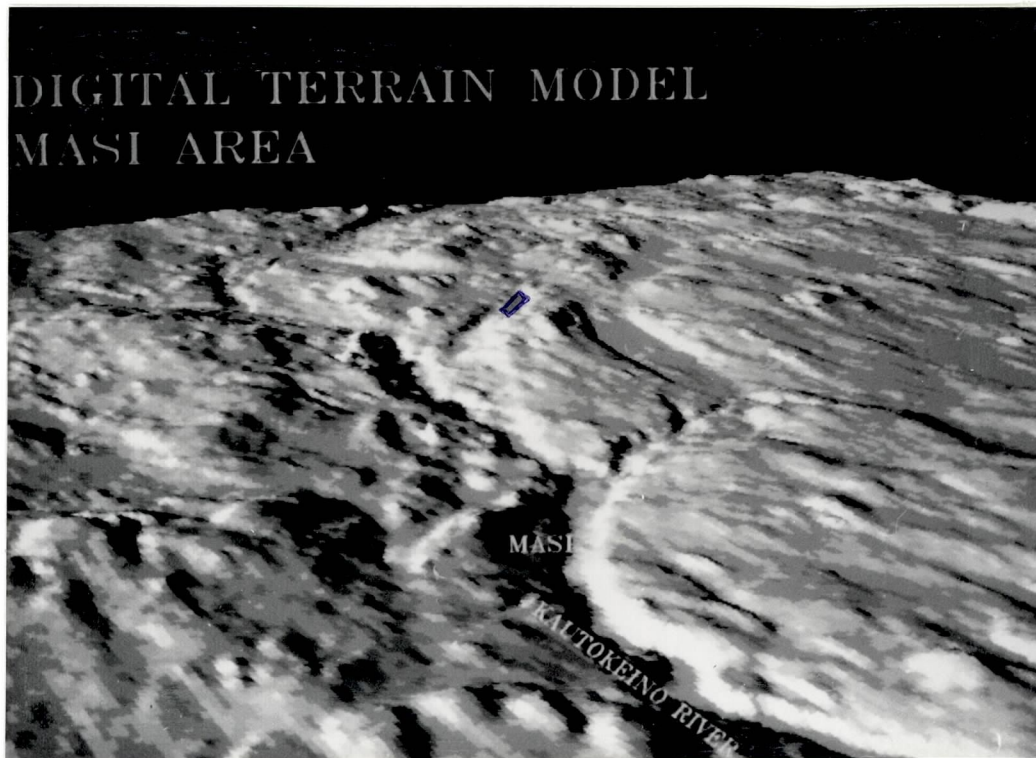


Fig. 13. A three-dimensional perspective model of the Masi area generated with the Erdas 3D module (Erdas 1990b). The vertical scale is exaggerated by a factor of 2. The view is towards the southwest along the MSFZ. The Biggevarri Duplex (Fig. 11) can be seen in the middle of the picture to the south of Masi. The rectangular grey-coloured area at the southern margin of the duplex structure has been investigated in detail by Olesen et al. (1990b).